Manaaki Whenua
Landcare Research

SedNetNZ, SLUI and contaminant generation.

Part 1: Sediment and water clarity

Prepared for: Horizons Regional Council

April 2018

SedNetNZ, SLUI and contaminant generation.

Part 1: Sediment and water clarity

Contract Report: LC3135

Les Basher, Raphael Spiekermann, John Dymond, Alex Herzig, Ella Hayman, Anne-Gaelle Ausseil

Manaaki Whenua – Landcare Research

Reviewed by:	*Approved for release by:*
Ian Lynn Capability Leader Manaaki Whenua – Landcare Research	Chris Phillips Portfolio Leader – Managing Land & Water Manaaki Whenua – Landcare Research

Contents

Summary

Project and client

Horizons Regional Council asked Manaaki Whenua – Landcare Research to document the use of SedNetNZ in the Horizons region; update the assessment of the impact of soil conservation work to date, and possible future work under the Sustainable Land Use Initiative (SLUI), on sediment load; assess the impact of SLUI works on water clarity; and update the assessment of the impact of climate change on sediment loads.

Objectives

- To document the history of SedNetNZ development and the various versions and calibrations that have been used in the Horizons region.
- To update SedNetNZ with the latest information on soil conservation works and farm plans under SLUI, and predict sediment outcomes based on SLUI work to date and for scenarios of future implementation.
- To re-run the analysis of impacts of climate change on sediment loads using down-scaled climate change scenarios for the Horizons region.
- To use SedNetNZ estimates of changes in sediment load to predict the outcome of changes in sediment load on water clarity.

Methods

- Previous reports to Horizons Regional Council were summarised focussing on the methodology and parameterisation of SedNetNZ.
- SedNetNZ estimates of sediment load were updated with the latest information on completed erosion mitigation works and new whole farm plans (WFPs) completed under the SLUI programme to December 2017, and predictions were made for two scenarios for future implementation of SLUI.
- Climate change impacts on sediment loads were predicted using the most recent regional climate model scenarios and a similar analytical method to previous work that predicted climate change impacts on sediment loads.
- The impact of SLUI on visual clarity in rivers was predicted from relationships between visual clarity, suspended sediment concentration (SSC) and sediment load.

Results

History of SedNetNZ

- SedNetNZ was implemented in the Manawatū catchment in 2013 as part of the Clean Water Productive Land research programme. This included data collection and analysis to underpin model development, and development of the algorithms and code for implementing surface erosion, landslide, gully, earthflow, bank erosion and deposition model routines.
- In 2014 SedNetNZ was used to undertake an assessment of the impact of SLUI works to date in the entire Horizons region and scenarios for possible future

implementation. It used the same parameterisation and algorithms as the 2013 analysis except for changes to sediment delivery ratio (SDR) and time period of active landsliding. The analysis suggested that:

  - scenario 4 (with targeting of priority farms and works) was always the best for reducing sediment loads, and sediment load reductions up to c. 60% could be achieved in the areas with the most highly erodible land
  - current implementation of farm plans (to 2013) in SLUI without any more new farm plans from 2014 onwards (scenario 0) would result in a 9% reduction in the annual sediment load in the Horizons region, but under scenario 4 a 32% reduction could be achieved
  - the most likely scenario (3) would result in a 27% reduction in sediment load.

- In 2015 Horizons requested an updated analysis of the impact of SLUI, using June 2015 WFP coverage and based on current implementation of farm plans in SLUI with no more new WFPs or works implementation from 2014 onwards. This was undertaken by interpolating the 2014 results through time rather than re-running the model. The results suggested the additional works would reduce sediment load by a further 200,000 tonnes per annum between 2004 and 2043.
- In 2015 SedNetNZ was used to predict the impact of climate change on sediment loads. Climate change scenarios were used to predict how changes in temperature will affect changes in storm rainfall and landsliding rates for three climate change scenarios. Calculated coefficients of change were used to update estimates of hillslope erosion from SedNetNZ. Climate change was predicted to increase sediment load between 10% (minor impact scenario) to 27% (major impact scenario) and therefore reduce the long-term effectiveness of SLUI.
- In 2017 a farm-scale version of SedNetNZ was produced using farm-scale Land Use Capability (LUC) mapping undertaken as part of SLUI. This produced an estimate of sediment load under grass for each LUC unit and can also be used to assess the effect of erosion mitigation. It utilises the farm-scale LUC polygons and will therefore capture the details of soil erosion at the farm scale, and is also useful for discussing soil conservation options with farmers LUC unit by unit. It generally cannot be used at a catchment scale because of a lack of whole-catchment farm-scale LUC mapping.
- SedNetNZ typically produces modelled suspended sediment yield (SSY) estimates within c. 40% of measured SSY, but in some cases there were large overestimates. Sensitivity analysis of SedNetNZ model parameters suggested an uncertainty of approximately ±50% (at the 95% confidence level) in estimates of sediment load, with the greatest uncertainty arising from the landslide probability density function, landslide SDR and gully density.

Updated SLUI analysis

An updated analysis of the effect of SLUI using 2017 WFP data showed that:

- SLUI works to date are estimated to have reduced sediment load by 835,000 tonnes (−6%). The greatest reductions (−18 to −19%) are predicted for the Kai Iwi, East Coast and Lower Rangitikei water management zones (WMZs).
- With no further WFP works (scenario 0), sediment reductions (as a percentage of sediment load) up to 2043 are proportional to the number of farm plans

implemented and will be greatest for the East Coast (−43%) and Tiraumea (−42%) WMZs. The largest sediment load reductions will be in the Lower Whangaehu (260,000 tonnes per annum, −34%), the Turakina (230,000 tonnes per annum, −30%) and Tiraumea (210,000 tonnes per annum, −42%) WMZs. The sediment load for the region is predicted to decrease by 16%.

- With ongoing implementation of WFP works (scenario 3), the greatest sediment reductions (as a percentage of sediment load) to 2043 are estimated to be in Middle Whangaehu (−62%) and Owahanga (−58%) WMZs. The reduction in sediment load for the region (−30%) will be twice that of scenario 0 with the greatest reductions in the Middle Whanganui (520,000 tonnes per annum, −49%), Lower Whangaehu (430,000 tonnes per annum, −55%), and Ohau (387,506 tonnes per annum, −51%) WMZs.

Effect of climate change

- Climate change is predicted to increase modelled sediment yields, with the extent of increase depending on the climate change scenario and varying spatially in response to variations in storminess.
- Increases in sediment load of >200% are predicted in some WMZs. The four climate change scenarios modelled produce region-wide increases in sediment load ranging from 41% to 179%. In order to offset these predicted large effects of climate change, continued − and arguably increased − investment in erosion mitigation will be vital.

Effect of SLUI on visual clarity

- The impact of SLUI on visual clarity is predicted to be significant, particularly for scenario 3.
- The current average median visual clarity at monitoring sites is 1.5 m, with 55% of sites having median values below this value, and a range from 5.0 m at the Waikawa at North Manakau Rd to 0.30 m at the Ohura at Tokorima site.
- Sixty-six of 124 Water Management Subzones (WMSZs) are predicted to have a reduction in SSC by 2043 as a consequence of SLUI.
- In the 29 WMSZs that are affected by SLUI, the average increase in visual clarity is 11% for scenario 0 and 29% for scenario 3. It is likely these increases are representative of the impact on SLUI for the remaining subzones with SLUI WFPs that do not have associated measurement sites.
- By 2043 the number of river sites with a visual clarity of >2 m is predicted to double under scenario 3.

Conclusions

- SedNetNZ has been used in multiple applications in the Horizons region since 2013. The model algorithms and parameterisation have largely remained the same, with subtle variations to SDR and time period of active landsliding.
- The farm-scale version can be used for discussing soil conservation options with farmers but has limited use at a catchment scale.

- SedNetNZ typically produces modelled SSY estimates within ±40% of measured SSY, but in some cases there were large overestimates.
- SLUI works carried out up to 2017 are estimated to have reduced total regional sediment load by 6%.
- With no further SLUI works it is estimated that by 2043 sediment load for the region will have decreased by 16%. However, with ongoing implementation of SLUI works (scenario 3) sediment load could be decreased by 30%.
- Climate change is predicted to increase sediment yields by 41% to 179% depending on the climate change scenario, which reinforces the need for ongoing SLUI works.
- SLUI works are predicted to increase mean visual clarity by between 11% (with no further SLUI works) and 29% (scenario 3).

Recommendations

- Now that good data are available on the location and area of erosion mitigation works, the analysis of the effect of SLUI erosion control works should be repeated using the area of these works rather than the area of WFPs to assess the effect of the difference between WFP area and implemented works area on modelled sediment load reductions from SLUI.
- Better data on the effectiveness of erosion mitigation at the whole-farm and whole-catchment scale are needed to test the erosion control effectiveness assumptions derived from hillslope-scale data. Horizons sediment load and farm plan works data could potentially be used for this analysis.
- The farm-scale version of SedNetNZ should not be used at the catchment scale because of a lack of whole-catchment or whole-erosion-terrain farm-scale LUC mapping.
- Continued investment in SLUI or other programmes for erosion mitigation will be required to offset the potentially severe effects of climate change.
- The reason(s) why SedNetNZ seriously overestimates sediment load in some catchments is not clear and requires further investigation.
- Current research will result in the replacement of the current surface and bank erosion models in SedNetNZ, and the present analysis should be repeated once these improvements have been made.

1 Introduction

Horizons Regional Council requested Manaaki Whenua – Landcare Research (MWLR) to document the use of SedNetNZ[1] in the Horizons region, and use SedNetNZ to provide updated assessments of the effect of the Sustainable Land Use Initiative (SLUI) on sediment load and visual clarity, the impact of climate change on sediment loads, and the impact of SLUI on phosphorus, nitrogen and *Escherichia coli* loads. :

The specific work components requested were as follows.

1 Document the development of SedNetNZ and the various versions and calibrations that have been used in the Horizons region, including the catchment-scale and farm-scale versions, and comment on in what circumstances they are appropriate for use and how accurate they are likely to be.

2 Update the SedNetNZ model with the latest information on soil conservation works completed and new farm plans that are part of the SLUI programme, and run the model to predict sediment outcomes based on SLUI work carried out to date and for scenarios of future implementation.

3 Re-run the analysis of the impacts of climate change on sediment loads using climate change scenarios from NIWA's[2] IPCC5[3] down-scaled climate change scenarios for the Horizons region.

4 Use SedNetNZ estimates of changes in sediment load with the methodology of Dymond et al. (2017) to predict the outcome of changes in sediment load on water clarity.

5 Extend the prediction of the outcomes from SLUI to include reduction in phosphorus, nitrogen and *E. coli* loads in rivers.

This report documents work completed for components 1 to 4.

2 Background

The origins and development of SedNetNZ are founded on the basis that moving from empirical sediment flux modelling to a model that incorporates erosion process information could provide a better basis for assessing the performance and targeting of erosion mitigation. Initial attempts at sediment flux modelling focused on widely available

[1] Throughout the text 'SedNetNZ' refers to the New Zealand version of the model, while 'SedNet' refers to the Australian version of the model.

[2] National Institute of Water and Atmospheric Research

[3] Intergovernmental Panel on Climate Change 5th Assessment Report

sediment yield[4] data for New Zealand rivers and found that the main driver for sediment yield is rainfall or runoff, and that there are regional differences that reflect variations in hydrologic regime and geology (e.g. Griffiths 1981, 1982; Hicks at al. 1996).

Subsequently, Hicks and Shankar (2003) and Hicks et al. (2011) utilised a comprehensive data set of sediment yield data from over 200 rivers to develop the Suspended Sediment Yield Estimator model (SSYE) to predict mean annual specific suspended sediment yield (SSY, $t \cdot km^{-2} \cdot a^{-1}$) based on a power function of mean annual rainfall (P) and an erosion terrain[5] classification (reflecting rock type, topography, and dominant type and severity of erosion processes):

$$SSY = aP^{1.7}$$

Values of a reflect erosion terrain groupings plus some regional adjustments. Hicks et al. (2011) note that the SSYE does not explicitly include the influence of land cover. The SSYE was released in 2002 by NIWA as a raster GIS data set with 100 m pixel resolution and incorporated into the Water Resources Explorer tool. It is currently available via NZ River Maps.[6]

Elliott et al. (2008) produced an alternative SPARROW[7]-based model calibrated using a similar sediment yield data set. This model relates SSY (at the scale of sub-catchments averaging c. 0.5 km^2) to mean annual rainfall (exponent of 2.02), slope, a simplified version of the erosion terrain classification, and land cover. The latter is scaled by comparison with SSY from forest and scrub, with pasture having an SSY 4.56 times higher than forest and scrub. This model is incorporated into the CLUES[8] modelling system.

Similarly, Dymond et al. (2010) developed the New Zealand Empirical Erosion Model (NZeem®) specifically to incorporate the effect of land cover on SSY. It has a similar form to the SSYE, but the value of the exponent is 2:

$$SSY = aCP^2$$

C was assumed to be 1 for woody vegetation and 10 for herbaceous vegetation or bare ground. Dymond et al. (2010) also used NZeem® to assess the effect on sediment yield of implementing soil conservation whole farm plans (WFPs) in the Manawatū catchment,

---

[4] 'Sediment yield' refers to sediment load per unit area ($t \cdot km^{-2} \cdot a^{-1}$), while sediment load refers to total mass of sediment generated ($t\ a^{-1}$).

[5] An erosion terrain is a land type with a unique combination of erosion processes and rates leading to characteristic sediment generation and yields (Page 2008). Erosion terrains were derived from New Zealand Land Resource Inventory data and are based on combinations of rock type/parent material, topography, rainfall, type, and severity of erosion processes. They were specifically developed to support the derivation of the SSYE.

[6] See https://shiny.niwa.co.nz/nzrivermaps/.

[7] **SPA**tially **R**eferenced **R**egression **O**n **W**atershed attributes (Alexander et al. 2004)

[8] Catchment Land Use for Environmental Sustainability – a catchment model developed to address the implications of land-use scenarios on stream water quality.

based on an assumption that a fully implemented farm plan would reduce SSY by 70% (largely based on Hawley & Dymond 1988, Hicks 1991, and Thompson & Luckman 1993). They also incorporated a methodology for assessing sediment delivery ratio (SDR) based on connectivity to the stream network.

NZeem® was subsequently used as a basis for developing tools for assessing the effectiveness of WFPs. Douglas et al. (2008) described an approach based on recalculating NZeem® sediment yields to account for the type of erosion mitigation (exotic forestry, space-planted trees in pasture, indigenous forestry/retirement), effectiveness in reducing erosion, treated area, and stage of maturity. Sediment export from any farm was calculated as the sum of sediment load from different land covers:

for exotic forestry $SSL_f = e_t \times (1 - M_f \times 0.9) \times A_f$

for pasture $SSL_p = e_p \times (1 - M_p \times 0.7) \times A_p$

for indigenous forestry $SSL_i = e_i \times (1 - M_i \times 0.9) \times A_r$

where:

$SSL_{f, p, i}$ = sediment load ($t \cdot a^{-1}$) for the respective land cover

e = the sediment load from NZeem® if the land was in pasture

M = maturity factor for the respective land cover

A = area of land treated with respective land cover.

Table 1 lists the sediment reduction percentages and maturity factors used in the analysis. This same approach was also advocated by McIvor et al. (2011) and Manderson et al. (2011). The sediment reduction percentages used in this early work remain the basis of erosion mitigation scenario analysis in SedNetNZ.

Table 1. Sediment reduction percentages and maturity factors used to assess WFP performance (from Douglas et al. 2008; McIvor et al. 2011)

Treatment	Sediment reduction (%)	Age to maturity	Maturity factor
Exotic forestry	90	20	M_f = age/20
Space-planted trees in pasture	70	15	$M_p = f \times$ age/15 (where f = proportion of trees that have survived)
Indigenous forestry/retirement			
Reverting pasture	90		0
Incomplete scrub canopy closure (early stage)			
Incomplete scrub canopy closure (intermediate stage, 3 years)	90		0.1
Complete scrub canopy closure (5 years)	90		0.5
Indigenous forest	90		1

Elliott and Basher (2011) reviewed the use of erosion models in New Zealand and commented that while erosion modelling is very mature overseas, many of the available models do not cover the range of processes relevant in New Zealand, particularly the wide variety of mass movement processes and complex gully-mass movement processes. In addition they suggested that the available models in New Zealand were not yet able to answer practical management questions. In particular, while the national-scale empirical sediment yield models capture a large degree of the variation in sediment yield across the country (Elliott et al. 2008; Dymond et al. 2010; Hicks et al. 2011), they do not give land managers information on the processes responsible for sediment generation to allow better targeting of erosion mitigation to the right places and contributing processes.

They concluded that a SedNet-type approach offers a middle ground between lumped empirical sediment yield models and detailed dynamic simulation models, which could better estimate the sediment yield from a wide variety of erosion processes and the effects of erosion mitigation on those sediment sources.

3 Objectives

- To document the development of SedNetNZ and the various versions and calibrations that have been used in the Horizons region, including the catchment-scale and farm-scale versions, and in what circumstances they are appropriate and how accurate they are likely to be.
- To update the SedNetNZ model with the latest information on soil conservation works completed and new farm plans that are part of the SLUI programme, and run the model to predict sediment outcomes based on SLUI work to date and for scenarios of future implementation.
- To re-run the analysis of impacts of climate change on sediment loads using climate change scenarios from NIWA's IPCC5 down-scaled climate change scenarios for the Horizons region.
- To use SedNetNZ estimates of changes in sediment load with the methodology of Dymond et al. (2017) to predict the outcome of changes in sediment load on water clarity.

4 Methods

4.1 SedNetNZ history

Previous reports to Horizons Regional Council were summarised focussing on the methodology and parameterisation of SedNetNZ. Scripts used in the various studies were compiled to assist with the description of the parameterisation and running of the model.

4.2 SedNetNZ scenario modelling with updated SLUI data

SedNetNZ estimates of sediment load were updated with the latest information on erosion mitigation works and new farm plans completed under the SLUI programme up to December 2017. SedNetNZ model estimates were updated using the same scripts and parameterisation as the previous Dymond et al. (2014) and Dymond and Manderson (2015) analysis and used to predict sediment outcomes based on work to date and the impact of possible scenarios of future farm plan and works implementation.

In contrast to Dymond et al. (2014), only two scenarios were analysed, as instructed by Horizons. For the sake of consistency, the naming of the scenarios here corresponds to that of Dymond et al. (2014):

- scenario 0: SLUI stops at the current level of implementation, with no new farm plans from 2018 onwards
- scenario 3: 35,000 ha of new plans per year; afforestation is not constrained.

For scenario 3, farm plans are allocated randomly to high-, moderate- and low-priority farms in the same proportions as in the past. In a similar fashion, the type of works is also allocated in the same proportions as in the past; i.e.:

- 50% afforestation
- 20% bush retirement
- 11% riparian retirement
- 12% space-planted trees
- 3% gully-tree planting.

The effect of farm plans is evaluated for each farm individually. Table 2 shows the effect of erosion control works in the farm plan. The afforestation and bush retirement effectiveness of 90% is based on published data (Dymond et al. 2010, 2016). The riparian retirement effectiveness is a conservative adjustment of the Australian 90% estimate of Prosser et al. (2001). The space-planted trees and gully tree planting effectiveness of 70% is based on published data (Hawley & Dymond 1988; Dymond et al. 2010).

Table 2. Effectiveness of erosion control works in reducing soil erosion at maturity and the required time to reach maturity

Erosion control treatment	Maturity (years)	Effectiveness
Afforestation	10	90%
Bush retirement	10	90%
Riparian retirement	2	80%
Space-planted trees	15	70%
Gully tree planting	15	70%

4.3 Impact of climate change on sediment loads

An assessment of the impact of climate change on sediment loads was undertaken using the most recent regional climate models, which provide the most detailed (5 km grid) predictions of changes to temperature and precipitation (see Pearce et al. 2016). Four scenarios, or representative concentration pathways (RCPs), are used to characterise a variety of trends depending on the approximate radiative forcing at 2100 relative to 1750:

- 2.6 W m^{-2} for RCP2.6
- 4.5 W m^{-2} for RCP4.5
- 6.0 W m^{-2} for RCP6.0
- 8.5 W m^{-2} for RCP8.5.

We used regional climate models for six general circulation models (GCMs) from the Coupled Model Inter-comparison Project (CMIP5).

The previous report by MWLR on modelling the impact of climate change on erosion rates and sediment loads for the Horizons region (Manderson et al. 2015) used the A1B (moderate impact), A1FI (fossil intensive representing a major impact), and a third 'minor impact' scenario, which was defined as a half-way point between the status quo and A1B. Manderson et al. (2015) made predictions based on the IPCC time period 2030–2049. The present work aims to complement the previous analysis by extending the horizon to assess the potential impact of climate change on sediment loads for the period 2081–2100, which is abbreviated as 2090, as well as using more detailed climate change predictions. Though the method used here is essentially the same as documented in Manderson et al. (2015), the climate change data used here is a significant improvement due to the regional downscaling of the models. The method uses two different approaches:

- In hill country dominated by landsliding predictions of the change in frequency of storms along with data on rainfall thresholds for landsliding and relationships between storm magnitude and landslide density (Reid and Page 2003) to determine a coefficient of change in landslide erosion with increasing temperature. The same coefficient of change was applied to four hillslope erosion processes (landslide, earthflow, gully and surficial erosion).
- In lowland areas surface erosion is the main erosion process, and the change in surface erosion was predicted from changes to mean annual rainfall using a similar coefficient of change approach.

The baseline sediment loads used to assess the effects of climate change are representative values of the long-term 20th century average and correspond to the 2004 column in Appendix 4 used for the SLUI scenario modelling (i.e. they do not incorporate the effects of SLUI). Appendix 5 provides a detailed description of the analysis of climate change impacts on sediment loads in the Horizons region.

4.4 Impact of SLUI on water clarity

Visual clarity of water is the distance (in metres) through the water column that objects can be seen. It is variable over time because it depends on suspended sediment concentration (SSC) which varies with river flow. Therefore, the median visual clarity is often used to characterise visual clarity at a site. When sediment loads in rivers are reduced through erosion mitigation, SSC in the river will also reduce and median visual clarity will increase (Dymond et al. 2017). The modelled reduction in SSC was calculated for each water management subzone according to the SLUI scenarios described in section 4.2.

To estimate the changes in visual clarity it is necessary to determine the relationship between visual clarity and SSC at each river site. Following Dymond et al. (2017), visual clarity (*v*) is related to SSC (*s*) by:

$$v = \exp(d)\, s^c \quad (1)$$

where *d* and *c* are constants at a given site. To determine *d* and *c*, concurrent measurements of *s* and *v* are plotted in log-log space and a straight line fitted to the data. Figure 1 provides an example of this for the measurement site at Mangawhero at Raupiu Road. The gradient of the line is *c* and the intercept is *d*.

$$\log(v) = d + c.\log(s) \quad (2)$$

If the sediment load at a river site is reduced as a fraction of the baseline sediment load (*frac*), then visual clarity will increase by the ratio $frac^c$. For example, if c = –0.5 and sediment load reduces by 40% (i.e. *frac* = 0.6), then visual clarity will increase by the ratio $0.6^{-0.5}$ = 1.3 (i.e. visual clarity will increase by 30%). Equation 2 was derived for different suspended sediment gauging sites and used to convert predictions of the effect of SLUI in reducing sediment load to predictions of the impact on visual clarity.

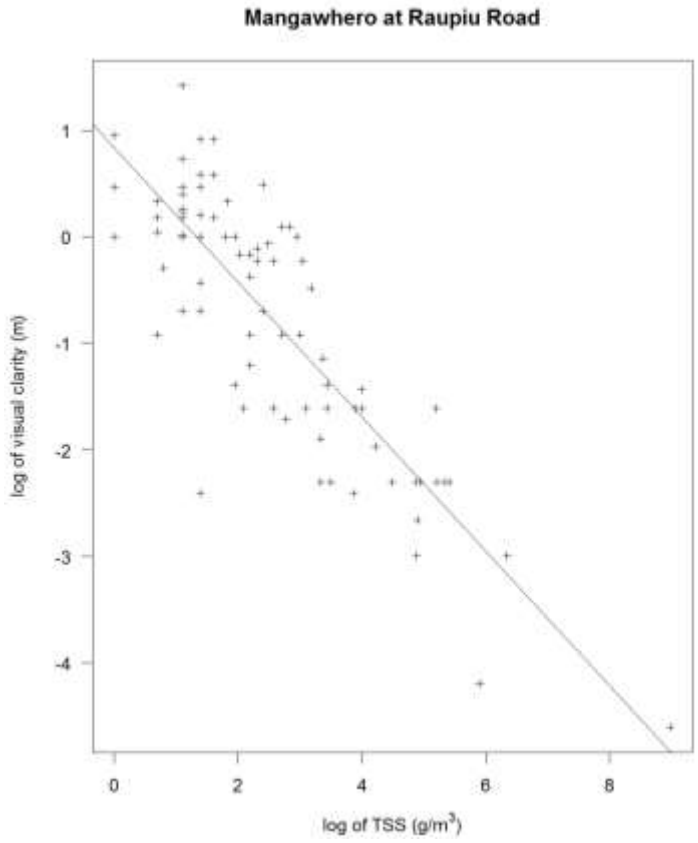

Figure 1. Relationship between visual clarity and suspended sediment concentration[9] at the Mangawhero at Raupiu Road measurement site.

5 History of SedNetNZ development and application in the Horizons region

5.1 Application of a simplified version of SedNet

The first attempt at assessing the potential reductions in sediment load of the Manawatū River associated with a range of different WFP scenarios is described in Schierlitz et al. (2006). This study used what is described as a simplified version of the SedNet model (Wilkinson et al. 2004) to predict sediment load. However, the data that were used to assess the WFP scenarios were from NZeem® modelling rather than a simplified SedNet. The approach used to analyse the WFP scenarios is similar to what is currently applied in SedNetNZ, with the assumption that fully implemented WFPs (mature space-planted poplars to control landsliding, or mature poplars and willows to control gully erosion)

[9] Note that most of Horizons measurements of suspended sediment concentration were based on analysis of total suspended solids (as in Figure. 1), which is likely to have underestimated SSC (see Hicks (2011) for a discussion of the difference between TSS and SSC). SSC is used here to refer to all analyses, whether based on SSC or TSS.

reduce erosion by 70% (Hawley & Dymond 1988; Hicks 1991, 1995; Thompson & Luckman 1993; see Table 1).

The results of this analysis were also used by Ausseil and Dymond (2008) to predict sediment concentrations for two indicative discharges (mean discharge and that which is exceeded 5% of the time) for three land-use scenarios: (1) indigenous vegetation, (2) present land use, and (3) implementation of 500 farm plans to predict how reductions in sediment load would affect water quality. This suggested the farm plan scenario would reduce sediment concentrations at mean discharge from 120 g m^{-3} to 58 g m^{-3} at Palmerston North.

5.2 Conceptual development of SedNetNZ

In recognition of the limitations of available empirical erosion models (SSYE, NZeem®, SPARROW) to represent individual erosion processes, and the high data and computing requirements for process-based, mechanistic erosion models (see Elliott & Basher 2011), MWLR decided to develop a hybrid empirical process-based model using the same structure as the Australian SedNet model (Wilkinson et al. 2004). SedNet is a sediment budget[10] model that predicts long-term average annual sediment load from individual erosion processes (including sheet, gully, streambank erosion, and floodplain deposition) and routes it down a stream network defined by stream links and associated catchments. However, the individual process models are empirical, with limited data input requirements, although there is a need for calibration data for the individual erosion process models.

SedNet provides a middle ground between the lumped empirical steady state erosion models and dynamic mechanistic simulation models, which gives it two other advantages. First, it is relatively easy to modify to incorporate a wide range of erosion processes (including mass movement processes that are very important in the New Zealand landscape). Furthermore, because of the model structure (being a node-link representation of the river network), it is relatively easy to accommodate improvements to individual model components or improved data availability (e.g. LiDAR-based digital elevation models – DEMs). A SedNet-type model requires a stream link and associated catchment polygon network, which is typically derived from a raster DEM. Sediment budgets are then calculated for each process in each stream link and associated sub-catchment, then routed downstream (Figure 2).

[10] A sediment budget characterises the sources, sinks and pathways of eroded materials within catchments.

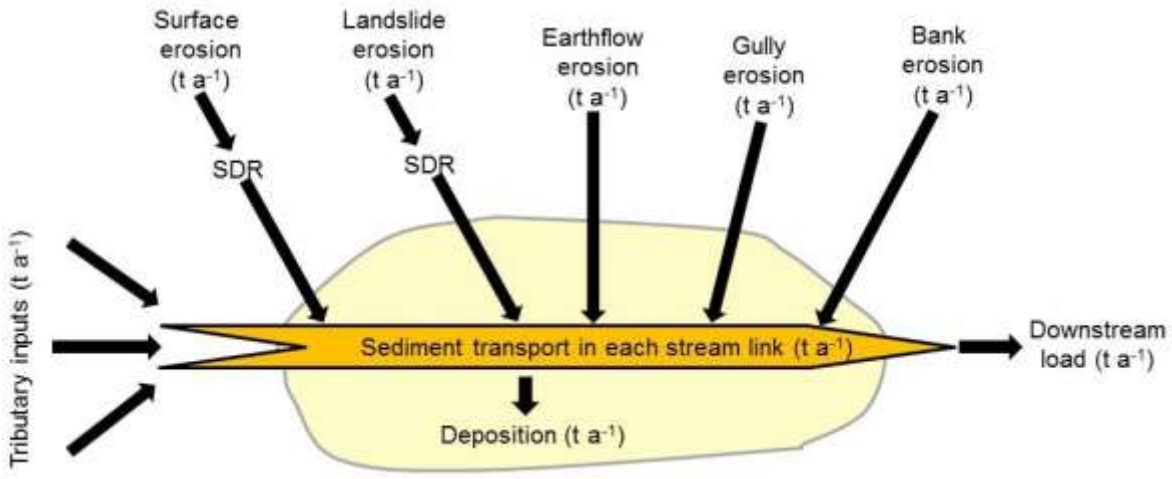

Figure 2. Conceptual structure of SedNetNZ

The strategy for developing SedNetNZ was described by Derose and Basher (2011a). They reviewed the implementation of SedNet in Australia and developed the conceptual approach for SedNetNZ. SedNet only considered input of sediment from the three main processes prevalent in Australian catchments – sheetwash (including rill erosion), gully erosion, and bank erosion – but it was recognised that in New Zealand there is a greater diversity of processes, and mass movement tends to dominate hillslope erosion. Much of the development of SedNetNZ focused on the development of models of these processes, collection of data to underpin model development, and the implementation of model code.

While SedNet has a sophisticated Graphical User Interface for data input, modelling and scenario analysis, Derose and Basher (2011a) suggested Python be used for model coding and that SedNetNZ could be developed as an ArcGIS toolbox. In the current implementation of SedNetNZ, pre-processing is done in ERDAS IMAGINE and ArcGIS, and the raster-based modelling is implemented in Python using the rios library (Raster I/O Simplification, http://rioshome.org/en/latest/), with evaluation, scenario analysis and visualisation in ArcGIS.

Derose and Basher (2011a) describe how nine key erosion process components of SedNetNZ could be developed: surface erosion, shallow landslides, large landslides, complex mass movement – gully erosion, tunnel gully erosion, earthflows, bank erosion, cliff erosion, and deposition. Details are given in Appendix 1. Derose and Basher (2011a) also included possible approaches to incorporate modelling of forestry roads and landings, and channel incision in bedrock, and discussed issues associated with bedload transport modelling, particle abrasion, modelling different particle size fractions, and assessment of model uncertainty using Monte Carlo approaches. The conceptual description of SedNetNZ in Derose & Basher (2011a) is largely what has been implemented in SedNetNZ and was published in Dymond et al. (2016). However, only models of landslide, gully, earthflow, sheet, and bank erosion have been implemented. A detailed description of the landslide component has also been published (Betts et al. 2017).

5.3 Implementation of SedNetNZ

SedNetNZ was implemented as part of the former Clean Water Productive Land research programme, largely following the recommendations in Derose & Basher (2011a), using the Manawatū catchment as a case study (Dymond et al. 2013a, 2013b). The case study had two components:

- data collection and analysis to underpin model development and provide information on critical source areas for sediment.
- development of the algorithms and code for implementation of SedNetNZ.

The SedNetNZ stream link and watershed network for the Manawatū was derived from a raster DEM (15 m pixel DEM derived from 20 m contours) using the ArcHydro extension in ArcGIS. To ensure consistency with NIWA's River Environment Classification (REC), the DEM was conditioned by 'burning' in the REC2 stream network[11]. For stream and catchment network derivation, a minimum catchment area was defined as 1 km^2 and produced an average catchment size of approximately 2 km^2 for the Manawatū. This resulted in a total of 3,093 sub-catchments.

Model algorithms were implemented for surface erosion, landslides, gullies, earthflows, bank erosion and deposition. Erosion terrains were used to define where to apply different model components spatially (see Appendix 2). The New Zealand Land Resource Inventory (NZLRI) data underpinning the erosion terrains was compiled at 1:50,000 scale, and are a generalisation of the pattern of different types of erosion (particularly gully and earthflow), and therefore have limited spatial resolution compared to the DEM and land cover data.

The model algorithms in this implementation of SedNetNZ largely followed recommendations in Derose & Basher (2011a) for surface erosion and landslide erosion (see Appendix 1), except that:

- a constant sediment delivery ratio (SDR) of 0.5 was incorporated into the surface erosion model component to account for the proportion of eroded soil that reaches a stream link
- a constant value of the soil erodibility factor (*K*) was used (0.25 for loam)
- a constant value of slope length (λ) of 200 m was used
- a different form of the landslide probability density relationship was used (compare Figure 3 with Figure 17 in Appendix 1; data are compiled in Appendix 3) with a single relationship for all rock types[12], which was derived from data collected at four sites in the Manawatū catchment (see Appendix 1 in Dymond et al. 2013b)
- a constant landslide depth (D) of 1 m is assumed.

[11] This ensures the stream link network is the same as REC2 but the sub-catchment network is not.

[12] Note that this does not match the landslide probability density function shown in Figure 4 of Dymond et al. (2013b), nor does the time period match (70 years in Dymond et al. (2013b), 20 years in the computer script).

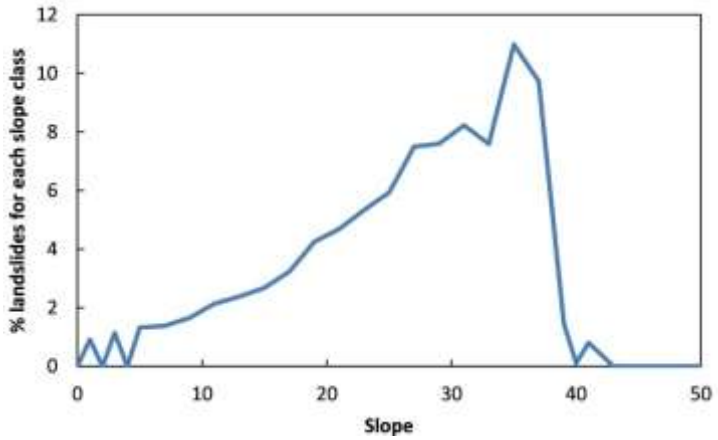

Figure 3. Probability–slope relationships for landslide-prone grassland hillslopes in North Island hill country The y axis shows the percentage (i.e. probability times 100) of land at the corresponding slope class that has experienced a landslide over a 20-year time period. The x axis shows slope angle in degrees.

Gully erosion (*GME*, t·km^{-2}·a^{-1}) was estimated using a slight modification of the equation suggested by Derose and Basher (2011a) for mass movement gully complexes:

$$GME = \frac{\rho \, \overline{A_g} \, \overline{GD}}{T}$$

where ρ is soil bulk density, $\overline{A_g}$ is the mean cross-sectional area of gullies, $\overline{GD}$ is mean gully density (km·km^{-2}), and T is the time since gully initiation. An SDR of 1 is assumed. Gully erosion was only calculated for erosion terrains prone to gully erosion (413, 642, 732, 742; see Appendix 2).

Similarly, earthflow erosion (*EE*, t·km^{-2}·a^{-1}) was estimated using a slight modification of the equation suggested by Derose and Basher (2011a):

$$EE = \rho \, \overline{M_e} \, \overline{D_e} \, \overline{ED}$$

where ρ is soil bulk density, $\overline{M_e}$ is mean speed of earthflows (m·a^{-1}), $\overline{D_e}$ is mean depth of earthflows (m), and $\overline{ED}$ is the mean density of earthflows in (m·km^{-2}). Earthflow erosion was only calculated for erosion terrains 632 and 633 (see Appendix 2).

Net bank erosion (BE_{net}) was estimated as a proportion of gross bank erosion (BE_{gross}):

$$BE_{net} = 0.2 \times BE_{gross}$$

$$BE_{gross} = M \times H$$

where BE is the volumetric rate of erosion per unit channel length (m^3·m^{-1}·a^{-1}), H is bank height (m), and M is bank migration rate (m a^{-1}). The relationship between net and gross bank erosion was derived from Derose and Basher (2011b) and accounts for accretion of eroded sediment in-channel. Riparian vegetation throughout the catchment was assumed to be grass. The relationship between bank migration rate and mean annual flood (Q_f) detailed in Derose & Basher (2011a) was used to predict M. Mean annual flood for each gauged Manawatū catchment was related to mean discharge ($\bar{q}$) as:

$$Q_f = a\,\bar{q}^b$$

where *a* and *b* are constants derived from the measured data. Mean discharge for each of the 3,093 subcatchments in the Manawatū was derived from WATYIELD (Fahey et al. 2010). Bank height was estimated from a regional relationship between bank height and mean discharge (Q_{mean}):

$$H = 2 + log_{10}Q_{mean}$$

Floodplain deposition rates were estimated separately for the major tributaries of the Manawatū: Mangahao, Mangatainoka, Tiraumea, Upper Manawatū, Oroua, and Pohangina rivers. For each tributary the proportion (*p*) of the total sediment load that overtops the banks (i.e. the sediment load carried in discharges exceeding bankfull discharge, defined as the discharge with return period of 1.5 years) was estimated from sediment discharge records. The total sediment deposited on floodplains for each tributary was estimated as the product of *p* and the total tributary sediment load. The annual rate of floodplain deposition ($t \cdot a^{-1}$) for a tributary was estimated by dividing the total deposited sediment by the area of flood plain in the tributary catchment (derived from the extent of floodplain in the erosion terrains). Where the tributary was controlled by flood-control banks (lower Manawatū), the deposition rate was set to 0.

Parameterisation of SedNetNZ was detailed in Dymond et al. (2013b), including a description of the data collection programme to support model development (see Table 3). Field data collection focused on the landslide, gully and earthflow components of SedNetNZ. Four representative study areas (windows) were selected to represent the erosion terrains characteristic of the Manawatū catchment:

- Pohangina, c. 3,705 ha, pastoral hilly steepland on unconsolidated sandstone, landslide-dominated with some gullying (erosion terrain 7.4.2)
- eastern Ruahine Ranges, c. 1,504 ha, steep forested mountain land on greywacke, landslide-dominated (erosion terrain 9.1.1)
- southeast Pahiatua, c. 1,010 ha, pastoral hill country on consolidated sandstone (erosion terrain 6.4.1) and mudstone (erosion terrain 6.3.1), landslide-dominated
- Mangamaire, c. 947 ha, pastoral hill country on mudstone, earthflow-dominated (most common erosion terrain is 6.3.2).

These windows were used to map erosion through time series air photo analysis and derive several parameters for model development and implementation, including landslide probability density functions, landslide depth, gully density, gully area, earthflow density, and earthflow depth. Full details of the data collection are given in Appendix 1 of Dymond et al. (2013b).

Table 3. List of parameter values used in implementing SedNetNZ for the Manawatū catchment (Dymond et al. 2013b, 2014)

Erosion process	Parameter	Parameter value (2013)	Parameter value (2014) where different to 2013
Surface erosion	α	1.2×10^{-3}	
	P	Derived from LENZ[a] mean annual rainfall layer	
	K	0.25	
	λ	200 m[b]	
	$\frac{dz}{dx}$	Derived from a 15 m cell size DEM	
	C	Bare ground 1.0 Pasture 0.01 Scrub, forest 0.005	
	SDR	0.5	
Landslides	ρ_{ls}	1.5 t·m^{-3}	
	$\overline{D}$	1.0 m	
	SDR_L	Defined for each erosion terrain (see Appendix 2)	
	LD	Slope dependent (Figure 3 and Appendix 3)	
	T	20 years	35 years
Gully	ρ	1.5 t·m^{3}	
	$\overline{A_g}$	900 m^2	
	$\overline{GD}$	0.22 km·km^{-2} for erosion terrains 413, 732, 642, and 742	
	T	100 years	
Earthflow	ρ	1.5 t·m^{-3}	
	$\overline{M_e}$	0.1.m·a^{-1}	
	$\overline{D_e}$	3.0 m	
	$\overline{ED}$	1024 m·km^{-2} for erosion terrains 632, 633	
Bank erosion	a	80	
	b	0.6	
Deposition	p	0.05	

[a] Land Environments of New Zealand – see https://www.landcareresearch.co.nz/resources/maps-satellites/lenz

[b] Note that this does not match the text in Dymond et al. (2013b), which suggests values of 200 m for stream density <2,000 m·km-^{2}, and for stream density >2000 m·km^{-2} there is an exponential decay of λ so that it is 100 m when stream density = 4,000 m·km^{-2}.

Results of the modelling were compared with measured sediment loads (Hicks & Hoyle 2012) and found generally to be in good agreement (most within ±40%), with the exception of the Pohangina and Tiraumea (Table 4). The modelling also allowed statements to be made about the relative contribution of different erosion processes in different sub-catchments. In the Upper Manawatū and the Tiraumea, landsliding was the

dominant process, whereas in the Oroua and Pohangina gully erosion was the dominant process.

Table 4. Comparison of SedNetZ modelled sediment loads and yields to measured values (from Hicks & Hoyle 2012)

River	Measured ($t \cdot a^{-1}$)	Modelled ($t \cdot a^{-1}$)	Measured ($t \cdot km^{-2} \cdot a^{-1}$)	Modelled ($t \cdot km^{-2} \cdot a^{-1}$)	Difference between modelled and measured[a]
Upper Manawatū at Hopelands	532,730	499,476	486	401	–17%
Manawatū at Teachers College	2,497,080	2,151,491	493	552	12
Mangahao at Ballance	102,620	120,750	668	454	–32
Mangatainoka at Pahiatua Town Bridge	55,020	133,593	139	338	143
Oroua at Almadale	313,780	291,881	718	996	39
Pohangina at Mais Reach	499,731	1,245,970	1,061	2,645	–1
Tiraumea at Ngaturi	286,860	552,016	439	752	71

[a] Expressed as % of measured load

5.4 Assessment of SLUI using SedNetNZ

SLUI is a voluntary programme that was implemented by Horizons to reduce hill country erosion in target catchments within the Manawatū –Wanganui region following the devastating effects of the 2004 storm. The availability of SedNetNZ provided an opportunity to use the model to assess the effects on river sediment loads of soil conservation works implemented under SLUI up to 2013, and assess the effects of potential future scenarios for SLUI implementation. It is reported in Dymond et al. (2014, 2016).

This work had three objectives:

6 to examine the calibration of SedNetNZ for the Manawatū catchment and calibrate it for the rest of the region

7 to down-scale SednetNZ to farm scale and run the implemented farm plan data to determine what reductions will be achieved at the 2013 level of implementation in 2043

8 to test five possible future implementation scenarios using actual and predicted farm plan implementation options for the Manawatū catchment and then the entire Horizons region.

The implementation of SedNetNZ across the entire Horizons region used the same stream link and watershed network, model algorithms and parameterisation as described in Dymond et al. (2013a, b), except that for the landslide model component SDR was set to 0.5 for all erosion terrains except the mountain lands (911 and 912), for which the SDR was

0.1 (see Appendix 2) and the time period (T) of active landsliding was set to 35 years (see Table 3).

Five different SLUI implementation scenarios were evaluated (Table 5). Farm plans were allocated randomly to high-, moderate- and low-priority farms in the same proportions as in the past (see section 4.2), and the type of works was also allocated in the same proportions as in the past: 50% is afforestation (except for scenario 2), 20% is bush retirement, 11% is riparian retirement, 12% is space-planted trees, and 3% is gully-tree planting. The effect of farm plans is evaluated for each farm individually using the values shown in Table 2 for the effectiveness of the erosion control treatment and maturity.

Dymond et al. (2014) note that the scenario analysis assumes that farm plans are appropriate for addressing soil erosion on highly erodible land (Page et al. 2005), and soil conservation works are maintained after implementation so that they represent the best-case scenario for implementation of WFPs. The analysis assumed that the reduction in sediment load due to the local application of erosion control works applied to the entire area of the WFP rather than just the area of erosion control works, because comprehensive data were not available on the location and area of erosion control works.

Table 5. Scenarios for future implementation of SLUI (Dymond et al. 2014)

Scenario	Area of new WFPs per year (ha)	Afforestation	Implementation
0	0	No new works	No new works
1	55,000	Yes	Following previous patterns
2	35,000	No	Following previous patterns
3	35,000	Yes	Following previous patterns
4	55,000	Yes	Optimised to priority farms

The modelled values of Dymond et al. (2014) are based on the re-calibrated SedNetNZ version, which relates the mapped landslide densities per erosion terrain to a 35-year period of active landsliding rather than 20 years. This resulted in overall slightly lower modelled sediment yields. Furthermore, to account for the effect of farm plans, individual erosion process rasters were summarised at the farm scale and mitigation effectiveness (Table 2) was applied at this scale. The resulting mean sediment yields were summarised per individual water management zone.

Modelled sediment loads are again compared with measured loads from Hicks & Hoyle (2012 -see Table 6). Dymond et al. (2014) note that there is generally good agreement between modelled and measured, apart from the Rangitikei at Pukeokahu, Rangitikei at Mangaweka, and Mangatainoka at Pahiatua Town Bridge. Further, they suggest that although there might be differences in modelled versus measured loads, the direction and magnitude of change as a result of SLUI should be well defined.

Table 6. Comparison of modelled sediment loads with measured sediment loads (from Dymond et al. 2014)

River	Years of record	Measured ($t \cdot a^{-1}$)	Modelled ($t \cdot a^{-1}$)	Difference between modelled and measured[a]
Manawatū at Hopelands	9.6	605,590	478,346	–21%
Manawatū at Teachers College	8.6	1,921,600	1,979,600	3%
Mangahao at Ballance	4.1	177,610	130,014	–27%
Mangatainoka at Pahiatua Town Bridge	4.3	55,090	148,771	170%
Oroua at Almadale	6.5	164,170	282,699	72%
Pohangina at Mais Reach	10.5	499,830	232,505	–53%
Makuri at Tuscan Hills	10.1	90,750	51,152	–44%
Tiraumea at Ngaturi	8.2	322,400	411,068	28%
Rangitikei at Mangaweka	8.1	592,750	1,533,840	159%
Rangitikei at Pukeokahu	11.3	30,750	422,058	1,273%
Whanganui at Te Rewa	11.4	3,322,120	3,684,090	11%
Ohura at NihoNiho	8.6	210,420	181,764	–14%
Owahanga at Branscombe Bridge	6.1	152,430	210,112	38%

[a] Expressed as % of measured load

The results of the analysis for changes in sediment load through time (in 5-year steps beginning in 2013) for the five different scenarios were compiled by water management zone. Relative (%) changes between 2004 and 2043 are given in Table 7. This analysis suggested that scenario 4 (with targeting of priority farms and works) was always the best for reducing sediment loads, and that sediment load reductions up to c. 60% could be achieved in the areas with the most highly erodible land.

Table 7. Percentage reductions in sediment load by 2043 for water management zones with SLUI farms (from Dymond et al. 2014)

Zone	Scenario 0	Scenario 1	Scenario 2	Scenario 3	Scenario 4
Akitio	–14	–49	–26	–45	–52
Cherry Grove	–3	–16	–7	–14	–18
Coastal Rangitikei	–11	–15	–16	–18	–24
East Coast	–42	–55	–51	–54	–55
Hopelands–Tiraumea	–6	–42	–11	–29	–28
Kai Iwi	–25	–51	–31	–50	–56
Lower Rangitikei	–24	–49	–39	–49	–53
Lower Whangaehu	–26	–53	–40	–50	–54
Lower Whanganui	–8	–23	–13	–23	–27
Mangatainoka	–3	–7	–4	–6	–9
Middle Manawatū	–13	–39	–29	–36	–45
Middle Rangitikei	–4	–18	–9	–17	–22
Middle Whangaehu	–13	–63	–44	–61	–63
Middle Whanganui	–6	–49	–19	–44	–49
Northern Coastal	–2	–42	–6	–35	–40
Oroua	–10	–38	–23	–34	–48
Owahanga	–13	–56	–25	–51	–58
Paetawa	–14	–41	–25	–36	–41
Pipiriki	–2	–23	–6	–19	–23
Tamaki–Hopelands	–6	–36	–19	–29	–36
Te Maire	–1	–42	–17	–34	–43
Tiraumea	–27	–51	–38	–45	–55
Turakina	–19	–47	–30	–45	–51
Upper Gorge	–2	–3	–2	–2	–3
Upper Manawatū	–4	–28	–15	–22	–33
Weber–Tamaki	–6	–17	–14	–16	–26

They conclude that the current implementation of farm plans in SLUI without any more new farm plans from 2014 onwards would result in a reduction of the annual sediment load in the Horizons region from 13.4 million to 12.2 million tonnes of sediment by 2043 (a 9% reduction). However, under scenario 4, which assumes 55,000 ha of new farm plans per year in priority order from 2014 on, without constraint on afforestation, there would be a reduction of the annual sediment load to 9.2 million tonnes by 2043 (a 32% reduction). Under the most likely scenario (3), which assumes 35,000 ha of new WFPs and no constraint on afforestation, the annual sediment load would reduce to 9.8 million tonnes by 2043 (a 27% reduction).

The results of this analysis were published by Dymond et al. (2016) and included an analysis of the effect of WFPs in reducing sediment load for the Manawatū catchment. There were also slight differences in model parameterisation, including:

- *LD* was expressed as expected density of landslides per year ($m^2 \cdot km^{-2} \cdot a^{-1}$) at slope angle *s* and renamed *f(s)* so that *LD* incorporated the time period for landsliding (described as 70 years)
- $\overline{ED}$ was reduced slightly (c.f. Table 3) to 1,000 $m \cdot km^{-2}$
- $\overline{GD}$ was reduced slightly to 200 (as a result of a change of units – originally expressed as 0.22 $km \cdot km^{-2}$ but changed to $m \cdot km^{-2}$).

5.5 2015 updated assessment of SLUI using SedNetNZ

In 2015 Horizons requested an updated analysis of the impact of SLUI using June 2015 WFP coverage, and based on scenario 0 of Dymond et al. (2014); i.e. current implementation of farm plans in SLUI with no more new WFP or works implementation from 2014 onwards. Scenario 0 results from Dymond et al. 2014 for 2013 and 2018 were interpolated linearly for 42 water management zones to calculate the equivalent sediment yield for the 2015 year and to project sediment yield out to 2043 (Dymond & Manderson 2015). Catchment coefficients for each period were calculated to express the relationship between WFP coverage and sediment yield, and used as a basis to extrapolate yield reductions from 2015 WFP coverage.

Coverage of WFPs had increased by approximately 72,560 ha since 2013 and resulted in an additional predicted reduction of sediment load of 200,000 $t \cdot a^{-1}$ between 2004 and 2043. Dymond and Manderson (2015) note that linear interpolation may slightly underestimate 2015 sediment yields because the full 2004–2043 curves of Dymond et al. (2014) tend to be sigmoidal. Similarly, they acknowledge that a limitation of the method used is that the average rate of sediment loss under WFPs within a catchment remains unchanged (i.e. the Dymond et al. (2014) rates are used). With fully spatial SedNetNZ modelling it is expected the degree of change will reflect variation in sediment yields between different landscapes and erosion terrains within a catchment. This limitation will become more pronounced as more WFPs are prepared for SLUI, and they recommended that the method was only suitable for interim estimates, and new full SedNetNZ modelling was strongly recommended for future reporting.

5.6 Farm-scale application of SedNetNZ

As part of the SLUI programme, extensive areas of farm-scale Land Use Capability (LUC) mapping have been undertaken in the Horizons region. This provides more detailed mapping of LUC than the NZLRI and has been used to develop a farm-scale version of SedNetNZ by applying the farm-scale mapping to develop a down-scaled erosion terrain coverage, which was then used to calculate sediment loads and yields (Dymond & Manderson 2016).

The NZLRI-based erosion terrain coverage was used to develop a set of rules to allocate farm-scale LUC units to the existing erosion terrain classes. The farm-scale mapping and a

sediment yield map at 1:50,000 scale[13] were intersected to calculate the sediment yield associated with each farm-scale LUC unit, with the constraint that sediment load from large areas (erosion terrains) are the same for farm-scale LUC and the 1:50,000 scale sediment yield map. The sediment load for each erosion terrain *i* (L_i, t·a^{-1}) was calculated as:

$$L_i = \sum_{j=1}^{n} a_{ij}\ Y_j$$

where Y_j is the average sediment yield (t·km^{-2}·a^{-1}) of erosion terrain *j* (as determined from the farm-scale LUC map and correlation), and a_{ij} is the area (km^2) of erosion terrain *j* (at farm scale) in erosion terrain *i* (at 1:50,000 scale). Values of a_{ij} were determined by overlaying a digital map of farm-scale LUC (converted to erosion terrains) with a digital map of NZLRI-based erosion terrains (at 1:50,000). L_i is determined by calculating the mean sediment yield for each erosion terrain (at 1:50,000) and multiplying by the area.

This produced a mean value of sediment yield (t·km^{-2}·a^{-1}) under grass for each NZLRI-scale erosion terrain (Table 8), which was used to calculate sediment load for each farm-scale LUC unit and to assess the effects of erosion mitigation as follows.

- Define sediment yield (t·km^{-2}·a^{-1}) for farm-scale LUC unit *x* (SSY_x) (Table 8).
- Define area (ha) in woody vegetation(A_w) and pasture (A_p) in LUC unit *x.*
- Calculate sediment load (t·a^{-1}) for area of pasture ($SL_{x,\,p}$) and woody vegetation ($SL_{x,\,w}$):

$$SL_{x,p} = SSY_x * A_p/100$$

$$SL_{x,w} = SSY_x * A_w * (1 - 0.9)/100$$

- Calculate total sediment load for LUC unit *x* (SL_x):

$$SL_x = SL_{x,p} + SL_{x,w}$$

- Assess effect of mitigation:
  - sediment load with soil conservation:

$$SL_{x,p,SC} = SY_{x,p} * 0.3$$

$$SL_{x,SC} = SL_{x,p,SC} + SL_{x,w}$$

  - sediment load with drainage works:

$$SL_{x,p,D} = SY_{x,p} * 0.5$$

$$SL_{x,D} = SL_{x,p,D} + SL_{x,w}$$

[13] In fact the sediment yield data were derived from raster-based (15 m pixel size) SedNetNZ modelling of hillslope erosion.

A shapefile was provided to Horizons, which contained the estimated sediment yield for each mapped farm-scale polygon (mean size 7.0 ha). The down-scaled SedNetNZ utilises the farm-scale LUC polygons and will therefore capture the details of soil erosion at the farm scale. It is useful for discussing soil conservation options with farmers, LUC unit by unit. The way it is down-scaled means that if up-scaled to whole catchments or erosion terrains it will be have the same sediment loads as the catchment-scale SedNetNZ. However, farm-scale mapping of LUC is generally not complete for whole erosion terrains or large catchments, so it is not generally practicable for use at these scales.

Table 8. Suspended sediment yield (SSY) under grass (t·km-2·a-1) for each erosion terrain and each associated LUC unit

Erosion terrain code	Erosion terrain description	SSY	LUC value in brackets = LUC Legend[a] p = partial inclusion (i.e. depending on rock type it may be split into other terrains)
111	Floodplains (contains some steep LUC with alluvium rock type)	146	1c 2 (10)p, 1w 1 (08), 1w 1 (10), 2c 1 (10)p, 2e 2 (10)p, 2s 1 (10), 2s 2 (10)p, 2s 5 (10), 2w 1 (08), 2w 1 (10), 2w 2 (10), 3c 1 (09), 3c 2 (10)p, 3e 4 (10)p, 3s 1 (10), 3w 1 (08), 3w 1 (09), 3w 1 (10), 3w 2 (08), 3w 2 (10), 3w 3 (08), 3w 3 (10)p, 3w 4 (10), 4e 4 (10)p, 4e 6 (10)p, 4s 2 (10), 4w 1 (08)p, 4w 1 (10)p, 4w 2 (09), 4w 2 (10), 4w 3 (10)p, 4w 5 (10)p, 5s 3 (10), 5w 1 (10), 6e13 (10)p, 6e14 (10)p, 6e16 (08)p, 6e28 (08)p, 6e28 (10)p, 6s 7 (10), 6w 1 (08)p, 6w 1 (10)p, 6w 2 (08), 6w 2 (10)p, 6w 3 (10), 7w 1 (10), 8e 3 (10)p, 8e 8 (10)p
211	Sand country	40	4e 6 (08), 4e10 (10), 6e14 (08), 6e24 (10), 6s 4 (10), 6s 5 (08), 7e14 (08), 7e15 (10), 8e 4 (08)
311	Peatland	20	3w 3 (10)p, 4w 1 (08)p, 4w 3 (10)p, 6e13 (10)p, 6e16 (08)p, 6e28 (10)p, 6w 1 (08)p, 6w 1 (09), 6w 1 (10)p, 6w 2 (10)p, 8w 1 (08)p, 8w 1 (10)p, 8w 2 (08)
411	Terraces and low fans, loess mantled	49	2s 2 (10)p, 3s 1 (08), 3s 4 (09), 6e28 (10)p
412	Terraces and low fans, young tephra, mostly pumiceous (Waimihia and younger)	126	3c 3 (10)p, 3e 8 (10), 3s 6 (10), 4c 2 (10), 4c 4 (10), 4e13 (10), 4s 3 (10), 4w 4 (10)
413	Terraces and low fans, infilled with Taupo tephra flow deposits—intensely gullied	243	6e26 (10), 7e19 (10), 8e 2 (10)p
414	Terraces and low fans, mid-aged (late Pleistocene/early Holocene) tephra, older tephra, or tephric loess	50	1c 2 (10)p, 1c 3 (10), 1w 2 (10), 2c 1 (08), 2c 1 (10)p, 2c 2 (10), 2c 3 (10), 2e 2 (10)p, 2s 3 (10), 2s 4 (10), 3c 1 (10), 3c 2 (10)p, 3c 3 (10)p, 3c 4 (10), 3s 2 (10)p, 3s 3 (10), 3s 4 (10), 4c 1 (10)
431	Terraces and low fans, gravelly	173	2s 1 (08), 3s 2 (08), 3s 2 (09), 3s 2 (10)p, 3s 3 (08), 3s 4 (08), 4s 1 (08), 4s 1 (10), 4s 4 (08), 6s 4 (08), 6s 6 (10), 7s 1 (08), 7s 3 (08), 8s 1 (08), 6s 6 (08)
511	Downland on loess	37	3e 1 (10)p, 3e 2 (08), 3e 3 (09), 3e 4 (10)p, 4e 1 (09), 4e 2 (08), 4e 2 (09), 4e 2 (10)p, 4e 4 (10)p, 4e 6 (10)p, 6e28 (10)p
512	Downland on Waimihia and younger tephra	93	3e 7 (10), 4e 8 (10)p, 4e 9 (10), 4e11 (10), 4e12 (10), 4w 5 (10)p, 6c 3 (08), 6c 3 (10), 6e28 (10)p
513	Downland on mid-aged tephra, older tephra, or tephric loess	65	3e 1 (08), 3e 1 (10)p, 3e 2 (10), 3e 3 (10), 3e 4 (10)p, 3e 5 (10)p, 4e 1 (08), 4e 1 (10), 4e 2 (10)p, 4e 3 (10)p, 4e 4 (10)p, 4e 5 (10)p, 4e 6 (10)p, 4e 7 (10), 4e 8 (08), 4e 8 (10)p, 4w 3 (10)p, 4w 5 (10)p, 5c 1 (10), 5c 2 (10), 5e 1 (10)p, 5s 2 (10), 6e28 (10)p
531	Downland on weathered sedimentary and non-tephric	75	3e 3 (08), 3e 5 (10)p, 4e 2 (10)p, 4e 3 (08), 4e 3 (10)p, 4e 4 (08), 4e 4 (10)p, 4e 5 (08), 4e 5 (10)p, 4e 6

Erosion terrain code	Erosion terrain description	SSY	LUC value in brackets = LUC Legend[a] p = partial inclusion (i.e. depending on rock type it may be split into other terrains)
	igneous rocks		(10)p, 4e 8 (10)p, 5e 1 (08)p, 5e 1 (10)p, 5e 3 (08)p, 5e 8 (08)p, 5s 2 (08), 6e16 (08)p, 6e28 (08)p, 6e28 (10)p
611	Hill country with loess	63	5e 1 (08)p, 5e 1 (10)p, 5e 3 (08)p, 6c 1 (09), 6e 1 (08), 6e 1 (09), 6e 2 (10)p, 6e 4 (08), 6e 5 (08)p, 6e16 (08)p, 6e28 (08)p, 6e28 (10)p
612	Hill country with shallow, young tephra	473	6e29 (10)p, 6s 2 (10), 6s 8 (10)p
613	Hill country with deep young airfall tephra	157	6e 3 (10)p, 6e18 (10), 6s 5 (10)
614	Hill country with mid-aged tephra	218	5e 2 (10)p, 6c 1 (10), 6c 2 (10)p, 6e 1 (10)p, 6e 3 (10)p, 6e 5 (10)p, 6e 6 (10)p, 6e 7 (10)p, 6e 9 (10), 6e23 (10)p, 6e25 (10), 6e28 (10)p, 6s 1 (10), 6s 8 (10)p
631	Hill country on mudstone	759	4w 1 (10)p, 5e 1 (08)p, 5e 1 (10)p, 5e 2 (10)p, 5e 8 (08)p, 6e 2 (08), 6e 3 (08), 6e 3 (10)p, 6e 4 (10)p, 6e 5 (10)p, 6e 7 (08), 6e 7 (10)p, 6e 8 (08), 6e 8 (10), 6e10 (10)p, 6e16 (08)p, 6e16 (10)p, 6e25 (08), 6e28 (08)p, 6e28 (10)p, 6e29 (10)p, 6w 2 (10)p, 7e 8 (10)p
632	Hill country on crushed mudstone/argillite with moderate earthflow-dominated erosion	6498	5e 1 (10)p, 5e 2 (10)p, 6e 1 (10)p, 6e 3 (10)p, 6e 4 (10)p, 6e 7 (10)p, 6e10 (08), 6e10 (10)p, 6e12 (08), 6e14 (10)p, 6e16 (08)p, 6e19 (10), 6e20 (10), 6e28 (10)p, 6e29 (10)p, 7e 8 (10)p
633	Hill country on crushed mudstone/argillite with severe earthflow-dominated erosion	19654	7e 6 (08), 7e 7 (08), 7e 8 (08), 7e 9 (08), 7e12 (10), 7e14 (10), 8e 3 (08)p
641	Hill country on cohesive sandstone	956	5e 1 (08)p, 5e 1 (10)p, 5e 2 (10)p, 5e 3 (08)p, 6c 2 (10)p, 6e 1 (10)p, 6e 2 (10)p, 6e 3 (10)p, 6e 4 (10)p, 6e 9 (08), 6e10 (10)p, 6e13 (10)p, 6e14 (10)p, 6e15 (08), 6e15 (10), 6e16 (08)p, 6e17 (10), 6e23 (10)p, 6e28 (08)p, 6e28 (10)p, 6e29 (10)p, 6s 2 (08)
642	Hill country on non-cohesive sandstone	1349	6e11 (10), 6e12 (10), 6e14 (10)p, 6e16 (08)p, 6e28 (08)p, 6e28 (09), 6e28 (10)p, 6e29 (10)p, 7e11 (10)p
651	Hill country on limestone	108	5c 1 (08), 5s 1 (08), 6c 1 (08), 6c 2 (08), 6e 5 (08)p, 6e16 (08)p, 6s 1 (08), 6s 9 (10)
661	Hill country on greywacke/argillite	649	5e 2 (08), 6c 2 (10)p, 6e 6 (09), 6e 6 (10)p, 6e 8 (09), 6e11 (08), 6e13 (10)p, 6e16 (08)p, 6e16 (10)p, 6s 3 (08)
662	Hill country on white argillite	109	6e 5 (08)p, 6e13 (08), 6e18 (08)
711	Hilly steeplands with shallow, young tephra	1182	7e 8 (10)p, 7s 1 (10)p
713	Hilly steeplands with mid-aged tephra	145	7e 8 (10)p

Erosion terrain code	Erosion terrain description	SSY	LUC value in brackets = LUC Legend[a] p = partial inclusion (i.e. depending on rock type it may be split into other terrains)
721	Hilly steeplands on volcanic rocks	225	7e 8 (10)p, 7e11 (10)p, 7s 1 (10)p, 8e 3 (10)p
731	Hilly steeplands on mudstone	4147	6e28 (10)p, 7e 1 (08), 7e 1 (10), 7e 2 (08), 7e 2 (10), 7e 7 (10), 7e 9 (10)p, 7e12 (08), 8e 1 (10), 8e 3 (10)p, 8e 8 (10)p
741	Hilly steeplands on cohesive sandstone	1954	6e16 (08)p, 6e28 (08)p, 6e28 (10)p, 7e 3 (10), 7e 4 (08), 7e 4 (10), 7e 5 (10), 7e 9 (10)p, 7e11 (10)p, 7e13 (10), 7e17 (10), 7e23 (10), 7s 2 (08), 7s 2 (10), 8e 1 (08), 8e 2 (08), 8e 2 (10)p, 8e 3 (08)p, 8e 3 (10)p, 8e 8 (10)p
742	Hilly steeplands on non-cohesive sandstone	1554	6e28 (10)p, 7e 6 (10)p, 7e16 (10), 8e 2 (10)p, 8e 3 (08)p, 8e 3 (10)p, 8e 8 (10)p
751	Hilly steeplands on limestone	1163	7e 3 (08)
761	Hilly steeplands on weathered greywacke/argillite	2082	6e16 (08)p, 6e28 (10)p, 7e 1 (09), 7e 2 (09), 7e 5 (08), 7e10 (08), 7e10 (10)
762	Hilly steeplands on unweathered white argillite	592	7e11 (08)
811	Upland plains/plateaux with tephra	85	6c 4 (10)
911	Mountain steepland on greywacke/argillite/younger sedimentary rocks with landslide erosion	2271	8e 3 (10)p, 8e 4 (10), 8e 8 (10)p, 8e 9 (10)
912	Mountain steepland on greywacke/argillite/younger sedimentary rocks with sheet/wind/scree erosion	841	6e27 (10), 7e21 (10), 7e22 (10), 8e 5 (10), 8e 6 (10), 8e 8 (10)p
921	Mountain steepland on volcanic rocks	96	7e11 (10)p

[a] 08 = southern Hawke's Bay Wairarapa; 09 = Wellington; 10 = Taranaki Manawatū

5.7 Climate change analysis

In the Manawatū–Wanganui region climate is predicted to become 2.1°C warmer by 2090, with related increases in rainfall (c. 16% more rain) and storminess (Ministry for the Environment 2008). Climate and erosion are closely linked, so there is a strong theoretical argument that increased temperature, rainfall and storminess will lead to increased rates of erosion and sediment yield.

Manderson et al. (2015) analysed the potential effects of climate change on sediment loads in the Horizons region. Down-scaled scenarios from the IPCC Fourth Climate Change Assessment, and climate−erosion relationships developed by Schierlitz (2008) and Petro (2013), were used to examine the implications of climate change on the outcomes of SLUI using SedNetNZ. The aim of this work was to estimate sediment yields for the Horizons region under four climate scenarios (no climate change, minor, moderate and major climate change), assuming that SLUI continues according to scenario 3 (see section 5.4) of Dymond et al. (2014). This section describes how SedNetNZ was used, while the analysis of climate change scenarios is more fully described in Appendix 5. The analytical approach was based on Petro (2013), who used NZeem® to do a similar analysis.

Climate change scenarios (see section 4.3 and Appendix 5) were used to predict how changes in temperature ($\Delta°C_x$) will affect changes in storm rainfall (R_x):

$$R_x = R + (\Delta°C_x \times j \times R)$$

where R is the current storm rainfall and j is a constant (0.078 – defined as the median increase in 3-hour storm rainfall for recurrence intervals ranging from 2 to 100 years). This was then used to predict how changes in storm rainfall will affect rates of landsliding. A linear relationship between landslide density (L, = number per kilometre) and storm rainfall (R) from the Gisborne area (Reid & Page 2003) was used to predict how changes in storm rainfall (using a threshold storm rainfall value for landsliding of 150 mm) change landslide density under the different climate change scenarios:

$$L_i = 0.73 \times R - 110$$

This equation was applied to predict landslide density for present storm rainfall and predicted increased storm rainfalls under climate change, and was then used to plot the effect of temperature increase on landslide density for 19 North Island rain gauge stations. The resultant relationships between temperature increase and landslide density were fitted by linear equations.

Equations from each linear plot were assigned to LENZ environments and multiplied across a reference sediment yield layer for each climate change scenario. This resulted in the creation of three 'coefficient of change' rasters that were used to update the landslide component of SedNetNZ. The same coefficient of change was applied to other hillslope erosion processes in hill country (earthflow, gully, surface erosion). In effect, the SedNetNZ results for each erosion process were modified by the coefficient of change for each climate change scenario. Results were aggregated to Horizons water management zones for comparison with the target SLUI management scenario.

Under all scenarios, climate change was projected to increase sediment loading in the region's rivers, ranging from 10% under the minor impact scenario to 27% under the major impact scenario. The rate of increase also varied by water management zone. The results suggested climate change would reduce the long-term effectiveness of SLUI, with the level of reduction under SLUI scenario 3 of 3.6 $Mt \cdot a^{-1}$ predicted to decrease to 2.6 $Mt \cdot a^{-1}$, 1.6 $Mt \cdot a^{-1}$ and 0.7 $Mt \cdot a^{-1}$ for the minor, moderate, and major impact climate scenarios, respectively. Adopting either SLUI management scenario 1 or 2 (Table 5) was predicted to improve long-term sediment reduction under climate change.

5.8 Uncertainty in SedNetNZ predictions

None of the contract reports address issues of uncertainty other than in the sense of comparison with measured sediment yields (Table 9). When applied only to the Manawatū catchment (Dymond et al. 2013a), modelled SSYs are on average 31% higher than measured SSYs, which is about double the standard error (%) on the measured SSYs (Hicks and Hoyle 2012). The modelled SSYs for the Mangatainoka (+143%) and Tiraumea (+71%) are much higher than the measured SSY. When applied to the entire region (Dymond et al. 2014), modelled SSYs are on average 120% more than measured SSYs, but this is mainly because of very large overestimates at three sites (Rangitikei at Managaweka: +159%, Rangitikei at Pukeokahu: +1,273%, Mangatainoka at Pahiatua Town Bridge: +170%). In summary, SedNetNZ typically produces modelled SSY estimates within c. 40% of measured SSY, but in some cases there are large overestimates. The reasons for this are not clear and require further investigation.

Table 9. Percentage difference between modelled and measured SSY (modelled as % of measured)

	Dymond et al. (2013a)	Dymond et al. (2014)
Manawatū at Hopelands	–17	–21
Manawatū at Teachers College	12	3
Mangahao at Ballance	–32	–27
Mangatainoka at PTB	143	170
Oroua at Almadale	39	72
Pohangina at Mais Reach	–1	–53
Tiraumea at Ngāturi	71	28
Makuri at Tuscan Hills		–44
Ohura at Nihoniho		–14
Owahanga at Branscombe Bridge		38
Rangitikei at Mangaweka		159
Rangitikei at Pukeokahu		1,273
Whanganui at Te Rewa		11

Dymond et al. (2016) provide a sensitivity analysis of SedNetNZ model parameters (Table 10). The contribution of each parameter to variance of catchment sediment load is

estimated using the calculus of partial differentials (illustrated in Appendix 1 of Dymond et al. 2016). The total variance is estimated to be approximately 256 × 10^9 $(t \cdot a^{-1})^2$, which gives a coefficient of variation of 0.24 and implies an uncertainty of approximately ±50% at the 95% confidence level. The greatest uncertainty arises from the landslide probability density function, landslide SDR, and gully density.

Table 10. List of model parameters, their estimated coefficient of variation, and resulting contribution to variance of catchment sediment load in (t·a-1)2 and percentage of variance of total catchment sediment load

Erosion process	Parameter	Coefficient of variation	Contribution to variance of catchment sediment load (× 10^9)
Surface erosion	α	0.025	0.07 (0.0%)
	P^2	0.05	0.27 (0.1%)
	K	0.05	0.27 (%0.1)
	L	0.2	4.4 (1.7%)
	F_s[a]	0.1	1.1 (0.4%)
	L	0.2	4.4. (1.7%)
	C	0.25	6.9 (2.7%)
Landslides	$\overline{D}$	0.05	3.8 (1.5%)
	SDR_L	0.2	60.8 (23.7%)
	LD f(s)	0.25	95.0 (37.1%)
Gully	$\overline{A_g}$	0.3	16.8 (6.6%)
	$\overline{GD}$	0.4	29.8 (11.7%)
	T	0.15	4.2 (1.6%)
Earthflow	$\overline{M_e}$	0.5	0.51 (0.2%)
	$\overline{D_e}$	0.25	0.12 (0.0%)
	$\overline{ED}$	0.2	0.08 (0.0%)
Bank erosion	*Mj*	0.5	5.5 (2.1%)
	Hj	0.25	1.4 (0.5%)
	Lj	0.025	0.01 (0.0%)
Floodplain deposition	p	0.3	0.93 (0.4%)
	SY_i	0.5	2.6 (1.0%)
	A_i	0.1	0.1 (0.0%)
All	ρ	0.07	21.5 (8.4%)
Total			**256 (100%)**

[a] Equal to the slope factor (S)

6 Updated assessment of SLUI using 2017 WFP data

Sediment loads modelled by SedNetNZ and incorporating SLUI works for the two different scenarios (0 and 3) are given in Appendix 4. The predicted loads are compiled for 5-year intervals. SLUI works to date (column SLUI-18 in Appendix 4) are estimated to have reduced sediment load by 835,000 tonnes, or 6% of the total load of the region's rivers. The greatest reduction (–18 to –19%) is predicted for the Kai Iwi, East Coast and Lower Rangitikei water management zones.

Figure 4 maps the percentage reduction in sediment loads achieved by 2043 by scenarios 0 and 3 for each water management zone in the Horizons region. It should be noted that the modelled reductions are based entirely on SLUI WFP coverage and associated works and do not account for other mitigating works achieved through other grants, private initiatives or land-use change. In common with previous work, it is also assumed that the erosion control reductions (Table 2) apply to the whole farm rather than just the area of land treated.

Currently there are no data that provide an assessment of the effectiveness of erosion mitigation at whole-farm, rather than hillslope, scale. Since the area of land treated by erosion control works is often a small proportion of total farm area, it is possible that the SedNetNZ modelled sediment load reductions may be an overestimate of sediment load reductions achieved by SLUI. Alternatively, it may be that applying the sediment load reductions just to areas where works have been implemented will underestimate reductions because SedNetNZ is not sufficiently detailed to map the critical source areas of erosion. To better assess the uncertainty in SedNetNZ predictions data on the effectiveness of erosion mitigation at whole-farm and whole-catchment scale is needed to compare with the hillslope-scale data (e.g. Hawley & Dymond 1988; Hicks 1991; Thompson & Luckman 1993).

The coloured dots in Figure 4 represent the location of farms where works have been implemented and are classified according to low-, medium- and high-priority farms, as farm plans implemented on high-priority farms are likely to have greater impact in reducing sediment yields than those on low-priority farms. The percentage reduction is proportional to the number of farm plans implemented per water management zone. Thus, for scenario 0 the greatest reduction achieved is for the East Coast (–43%) and Tiraumea (–42%) water management zones, whereas for scenario 3 the greatest reduction by 2043 is in the Middle Whangaehu (–62%) and Owahanga (-58%) water management zones.

Table 11 lists the percentage reductions that are displayed in Figure 4. By 2028 all high-priority farms have been targeted by SLUI. After 2029 the remaining low- and moderate-priority farms are targeted. The rate at which sediment loads are decreased is therefore not as rapid as before 2029. Furthermore, the percentage reduction differs depending on the number of farm plans in a water management zone. For example, up until 2017 very few farm plans had been implemented in the Middle Whanganui water management zone, and primarily on medium-priority farms. Thus the reduction in scenario 0 was 9% based on works completed by 2017. However, as Figure 4 shows, the majority of remaining farm plans are implemented in scenario 3 after 2017, leading to a reduction of 49% by 2043.

Table 11. Percentage reductions in sediment loads by 2043 for water management zones where SLUI farm plans have been implemented

Water management zone	Scenario 0	Scenario 3
Middle Whangaehu	–33	–62
Owahanga	–34	–58
East Coast	–43	–57
Lower Whangaehu	–34	–55
Tiraumea	–42	–55
Kai Iwi	–35	–54
Lower Rangitikei	–38	–51
Turakina	–30	–51
Akitio	–28	–50
Middle Whanganui	–9	–49
Middle Manawatū	–31	–46
Te Maire	–13	–42
Northern Coastal	–6	–40
Manawatū Tamaki Confluence to Hopelands	–27	–40
Oroua	–21	–37
Paetawa	–18	–35
Upper Manawatū	–14	–33
Manawatū Hopelands to Tiraumea Confluence	–11	–32
Lower Whanganui	–16	–27
Coastal Rangitikei	–14	–26
Manawatū Weber Road to Tamaki Confluence	–12	–25
Pipiriki	–5	–23
Middle Rangitikei	–8	–20
Cherry Grove	–5	–16
Mowhanau	–11	–15
Mangatainoka	–5	–8
Upper Gorge	–2	–2

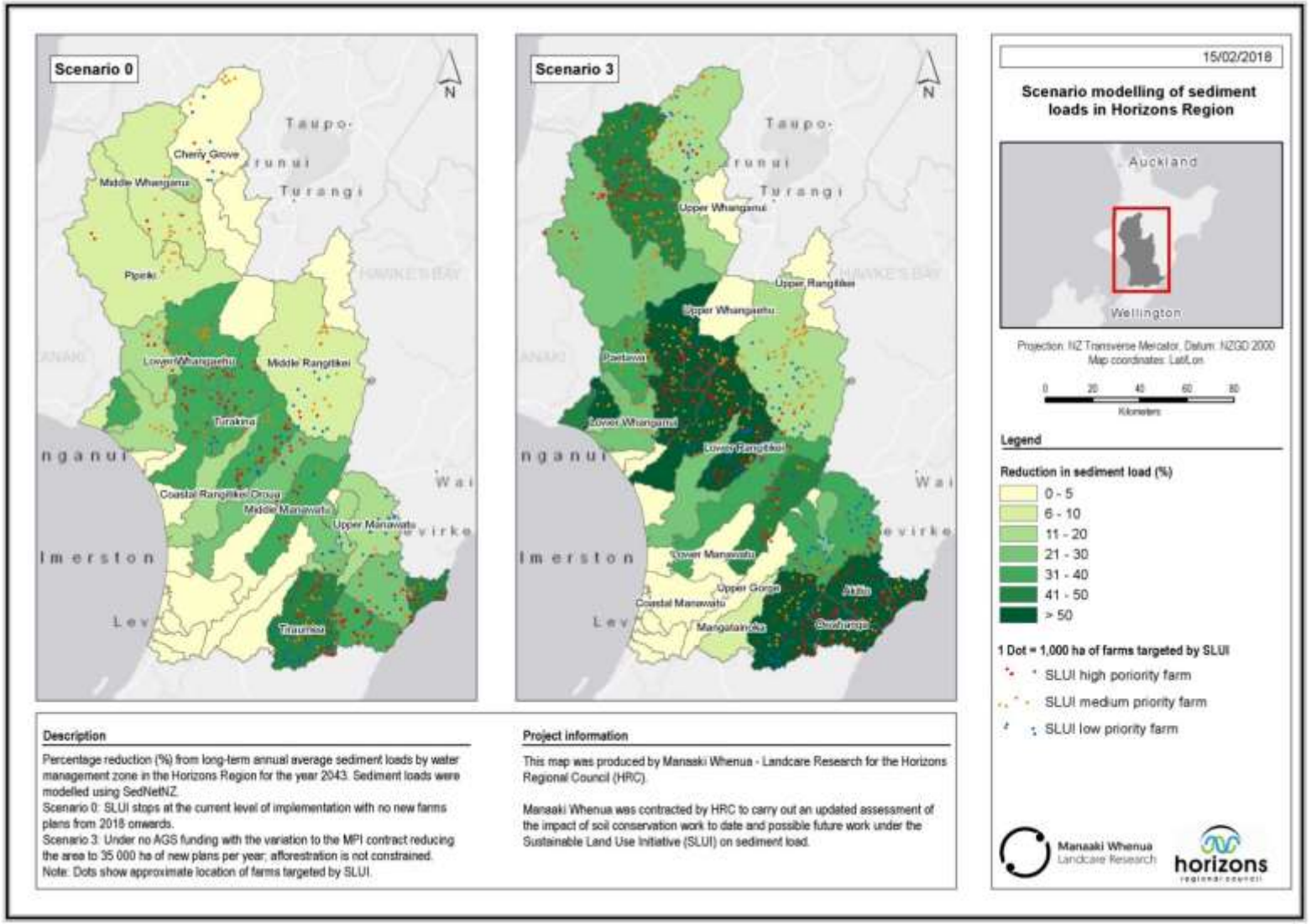

Figure 4. Map showing percentage reductions of annual sediment loads for scenarios 0 and 3, by water management zone

6.1 Scenario 0

Scenario 0 assumes that SLUI works cease at the current level of implementation at the end of 2017. Thus the works reach their final level of maturity by the year 2033 (see Table 2) with no further reduction in sediment loads between 2033 and 2043. These reductions are graphed in Figures 5 to 7.

In terms of reduction in sediment loads, the Lower Whangaehu water management zones is predicted to have the most significant reductions at 260,000 $t \cdot a^{-1}$ (–34%), closely followed by the Turakina (230,000 $t \cdot a^{-1}$, –30%) and Tiraumea (210,000 $t \cdot a^{-1}$, –42%) water management zones. For the Horizons region as a whole, the sediment load is predicted to decrease from 13.4 × 10^6 $t \cdot a^{-1}$ to 11.3 × 10^6 $t \cdot a^{-1}$, which equates to a reduction of 16%.

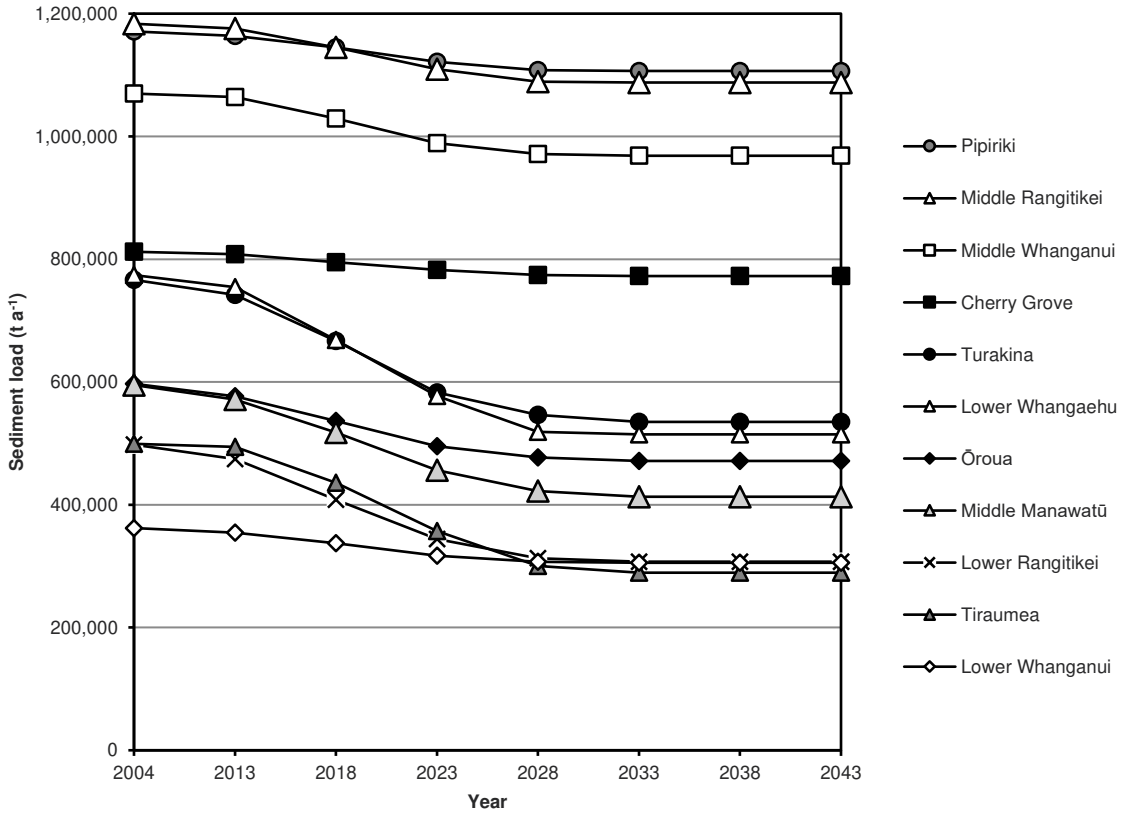

Figure 5. Sediment loads (t·a–1) in scenario 0 for the water management zones in SLUI with the highest loads, 2004 to 2043.

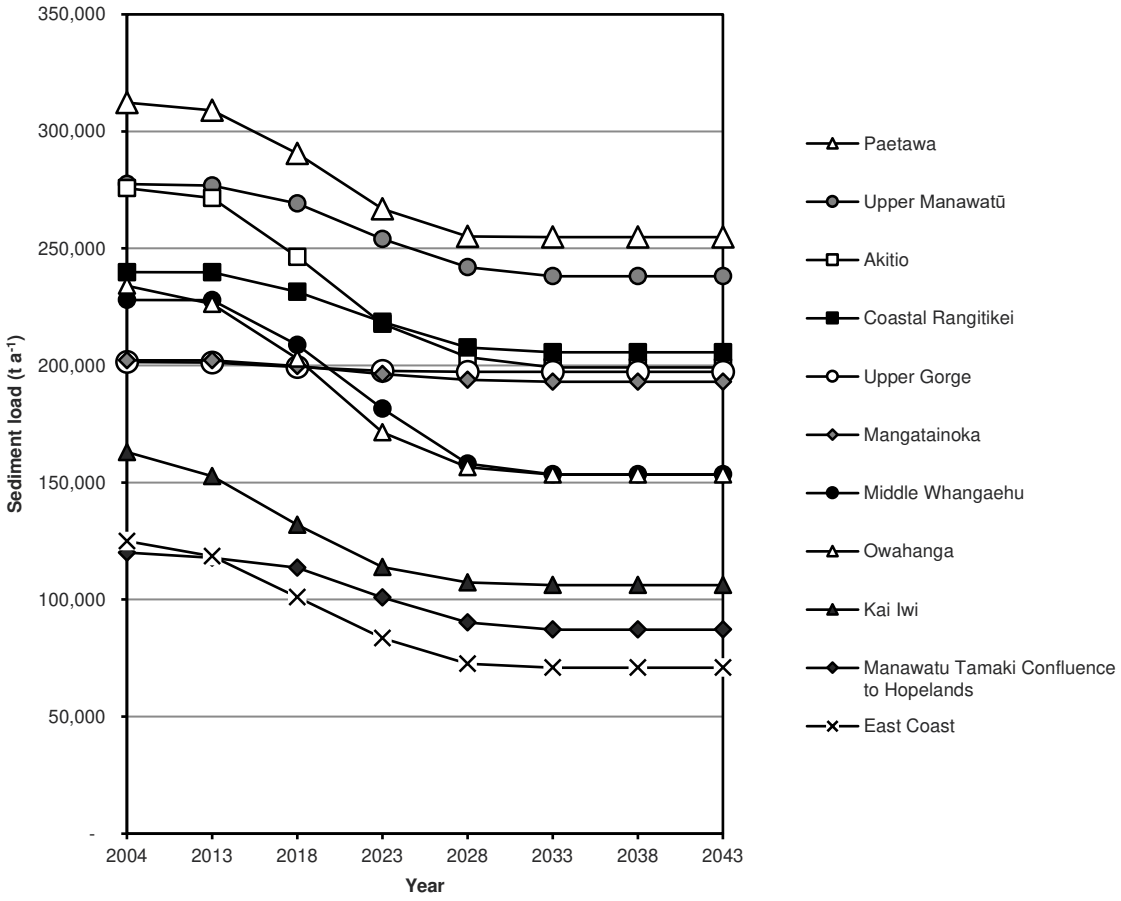

Figure 6 Sediment loads (t·a–1) in scenario 0 for the water management zones in SLUI with moderate loads, 2004 to 2043.

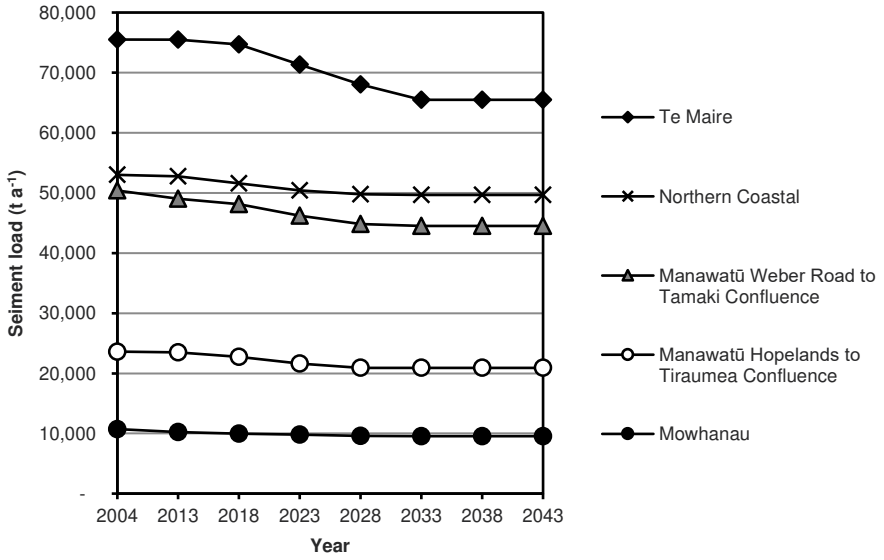

Figure 7. Sediment loads (t·a–1) in scenario 0 for the water management zones in SLUI with low loads, 2004 to 2043.

6.2 Scenario 3

Due to the continuation of SLUI in scenario 3 and associated implementation of farm plans at the same rate as in the past, the impact on reducing sediment loads is much greater. These reductions are graphed in Figures 8 to 10. It is immediately apparent that many of the curves are much steeper than those in Figures 5 to 7. The reduction in sediment load achieved is twice that of scenario 0, at $4.1 \times 10^6 \cdot t \cdot a^{-1}$, which is a decrease of 30%. When excluding water management zones outside the SLUI footprint, the reduction increases to 37%. The water management zones with the greatest reductions in sediment loads are the Middle Whanganui (520,000 $t \cdot a^{-1}$, –49%), Lower Whangaehu (430,000 $t \cdot a^{-1}$, –55%), and Ohau (387,506 $t \cdot a^{-1}$, –51%).

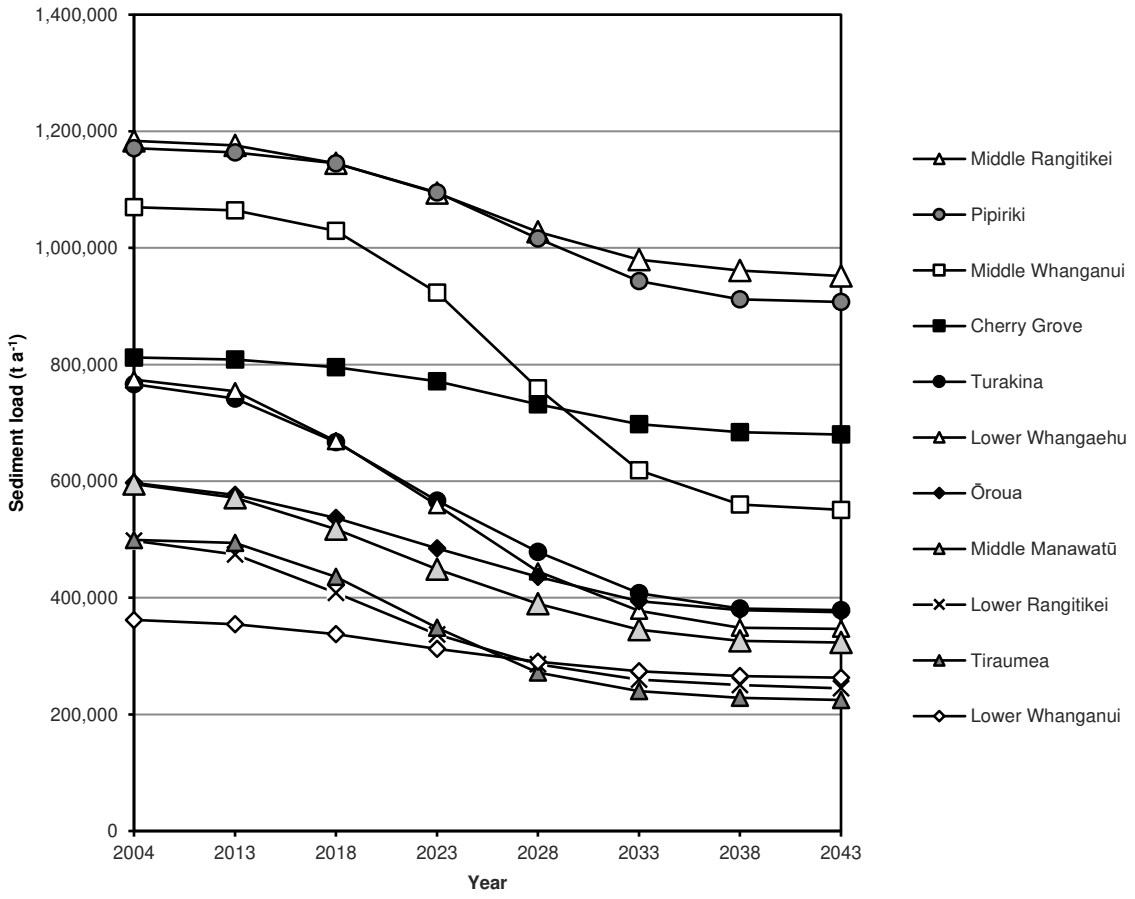

Figure 8. Sediment loads (t·a-1) in scenario 3 for the water management zones in SLUI with highest sediment loads, 2004 to 2043.

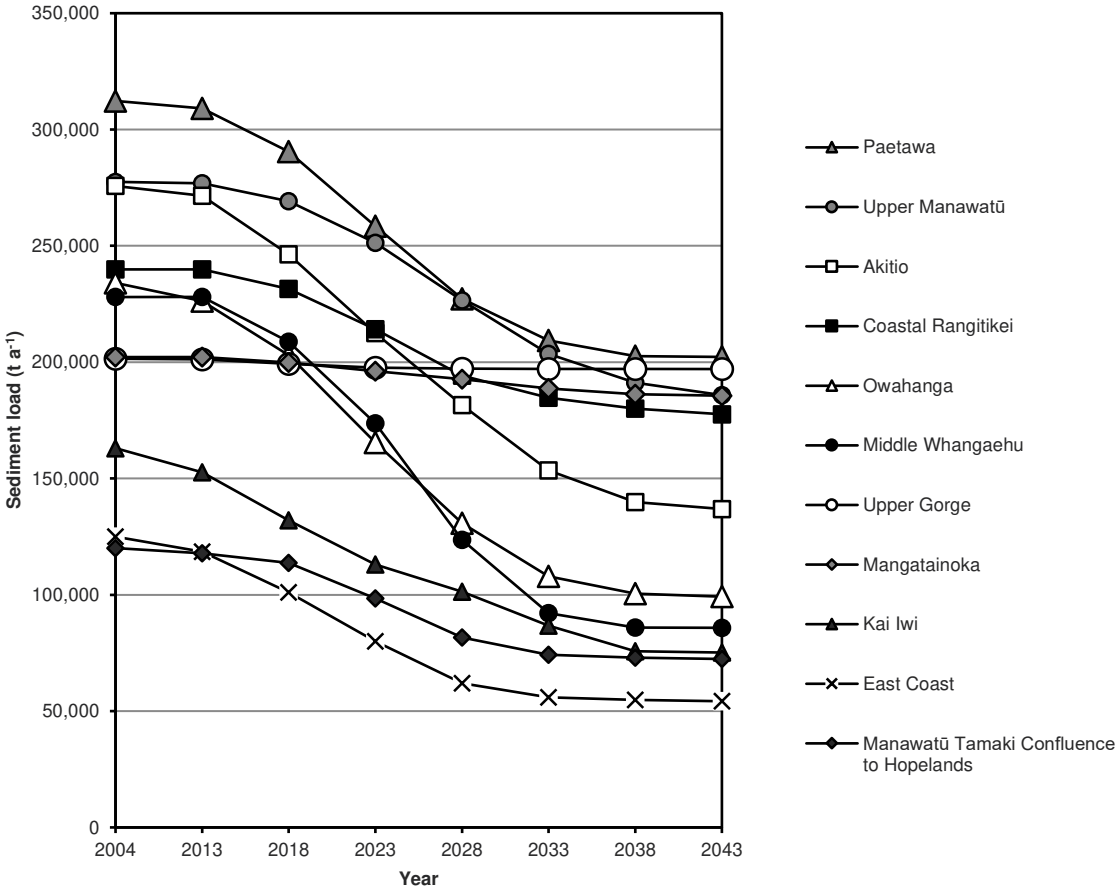

Figure 9. Sediment loads (t·a-1) in scenario 3 for the water management zones in SLUI with moderate loads, 2004 to 2043.

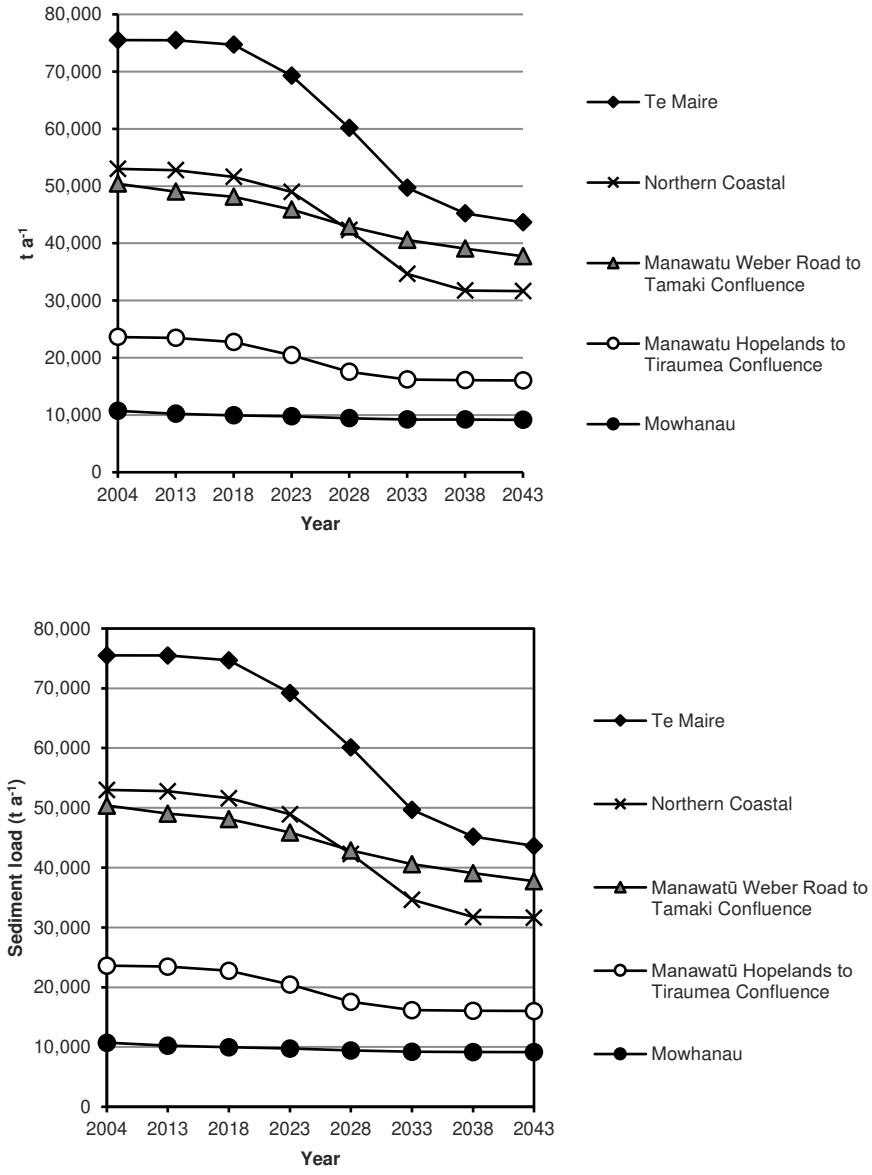

Figure 10. Sediment loads (t·a-1) in scenario 3 for the water management zones in SLUI with low loads, 2004 to 2043.

7 Impact of climate change on sediment loads

Figures 11 and 12 provide an overview of the projected increase to sediment loads in the Horizon region's rivers from the baseline modelled by SedNetNZ, based on the coefficient of change approach method described in section 4.3. The four maps in Figure 12 show the four projected scenarios for the end of the 21st century based on the RCPs described in section 4.3. Appendix 5 tabulates the full results, calculated as the average of the six GCMs used for each of the four RCPs. The size of the circle in Figure 12 shows the degree to which the six GCMs are in agreement: the larger the circle, the greater the range.

The strong overall increase of modelled sediment yields is directly related to the predicted increase in radiative forcing ($W \cdot m^{-2}$), which the different scenarios depict. As a

consequence of the enhanced greenhouse effect, the additional energy uptake by the Earth's atmosphere increases the frequency and magnitude of rainfall events. The results provide a compelling representation of the impact an increase in storminess is predicted to have on sediment yields.

There is a significant difference in the modelled results of the climate scenarios, depending on the RCP used (see Figures 11 and 12). RCPs 4.5 and 6.0 (see Moss et al. 2010) are scenarios that stabilise after 2100 and were not previously considered by Manderson et al. (2015). In these more moderate scenarios, changes to sediment yields are predicted to double east of the ranges and in the Whanganui catchment. In the RCP 6.0 scenario, modelling results in the Middle Whanganui water management zone show an increase in sediment yields of more than 200%. The only decrease is found in the smaller west coast catchments, where annual precipitation is predicted to decrease by the end of the century, which will lead to reduced rates of surficial erosion. If the results presented in Figure 12 and Appendix 5 accurately characterise the expected changes to sediment yields by 2090, the consequences would be drastic and would require radical mitigation options in order to adapt effectively.

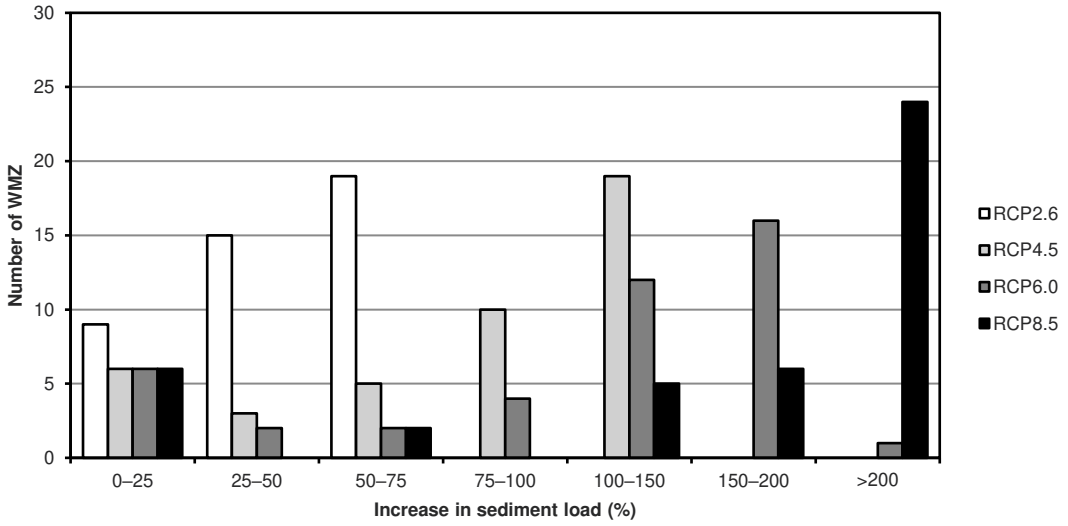

Figure 11. Modelled changes to sediment loads (%) of water management zones (WMZ) in the Horizons region due to climate change at c. 2090 according to the four RCPs.

In contrast to Manderson et al. (2015), we have characterised the climate change impacts at the end of the century rather than mid-century, since the trends of the various RCPs become more evident as the radiative forcing in the different RCPs diverge appreciably after 2035 and the RCPs follow similar trends to the IPCC Fourth Climate Change Assessment scenarios up to around 2040 (see Figure 19 in Appendix 5). For this reason, an analysis using the more recent RCPs for the period 2030-2050 would render very similar results to that of Manderson et al. (2015). According to Manderson et al. (2015), the A1B scenario (comparable to RCP6.0) would result in a 20.8% increase in sediment load by 2040 and A1F1 (comparable to RCP8.5) would result in a 29.6% increase. The modelled sediment reduction for SLUI Scenario 3 is 4.1 Mt a^{-1} by 2043, which is a 30% reduction. Therefore, SLUI Scenario 3 would be effective at countering the increase in sediment load

due to climate change up to ~2043. However, the long-term impacts of climate change (~2090) are unlikely to be mitigated under current SLUI targets.

The results are an indication of the trend, and the interpretation of the results requires careful consideration of the underlying assumptions of the modelling process.

- The adjustment for estimating the change in heavy rainfall per 1°C temperature increase is 7.8%.
- This adjustment can be applied to historical rainfall records to predict the change in magnitude and frequency of future rainfall events.
- A set of meteorological sites can be used to adequately characterise responses of different land environments (i.e. LENZ classes – see Appendix 5).
- Most importantly, the relationship between landslide density and storminess identified by Reid and Page (2003) in the Te Arai land system within the Waipaoa catchment can be applied to the landscape in the Horizons region.
- The factors of change established for the dominant erosion processes in hill country (landslide erosion) and lowland areas (surficial) adequately represent the expected change due to climate change, and for the other (non-dominant) erosion processes modelled by SedNetNZ (i.e. earthflow and gully erosion).

Notwithstanding these limitations of the climate change analysis, the results provide substantial evidence that rainfall events towards the end of the 21st century will increase in frequency and magnitude and will almost certainly lead to a significant increase in rates of erosion in the hill country of the Horizons region. Careful consideration and (long-term) planning is required to mitigate the impact of climate change. Past and future efforts of the SLUI, including the scenarios modelled here (see section 6), are essential if the impact of climate change is to be minimised. To ensure the vulnerable landscapes of the Horizons region can cope with the expected increases in erosion-triggering events, further mechanisms by which adaptation can be better achieved will require further research and careful mitigation planning.

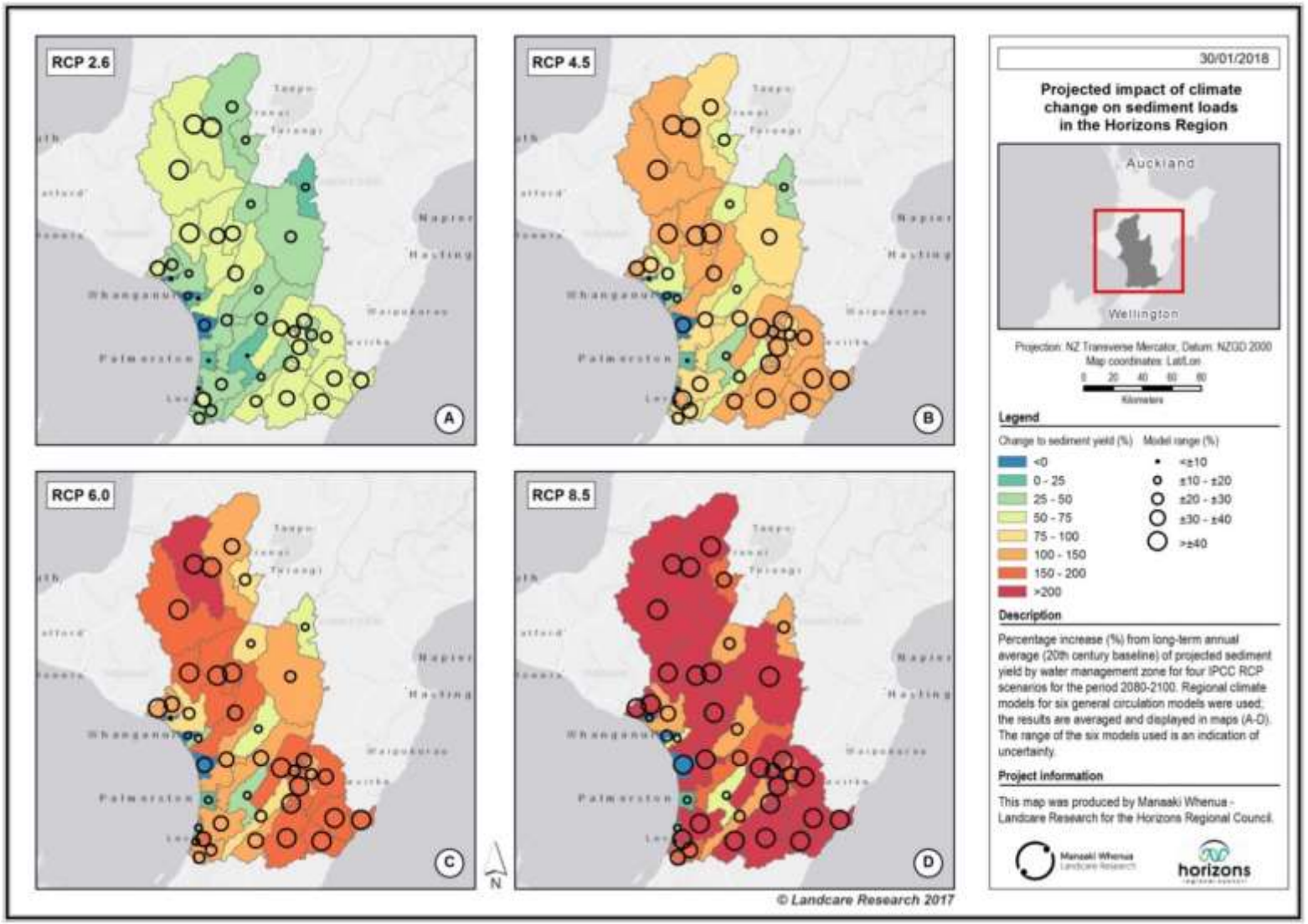

Figure 12. Projected impact of climate change (c. 2090) on sediment loads.

8 Impact of SLUI on water clarity

It is assumed that the modelled reductions in sediment yields and relative increase in visual clarity established using relationships at the measurement sites can be used as an approximation for the impact of SLUI for rivers upstream of the measurement sites. Results for water management zones are limited to those that have an associated measurement site and can therefore only be related to water management subzones. Figure 13 shows median visual clarity of sub-catchments in the Horizons region and the predicted impact of SLUI scenarios 0 and 3 by 2043 while Figure 14 displays this spatially. Appendix 6 tabulates the current median water clarity for the 84 measurement sites and associated water management zones and subzones (Table 17), and the predicted median water clarity in 2043 for scenarios 0 and 3 for those water management zones impacted by SLUI WFPs (Table 18). Figure 14 shows median visual clarity of rivers at measurement sites, and the predicted increase associated with scenarios 0 and 3 for SLUI implementation to 2043. Improved visual clarity only occurs at measurement sites where SLUI works are implemented in the catchments upstream. The increase in visual clarity is based on the relationship between visual clarity and suspended sediment concentration established for each river site (described in section 4.4 – data for intercept *d* and gradient *c* are compiled in Table 17).

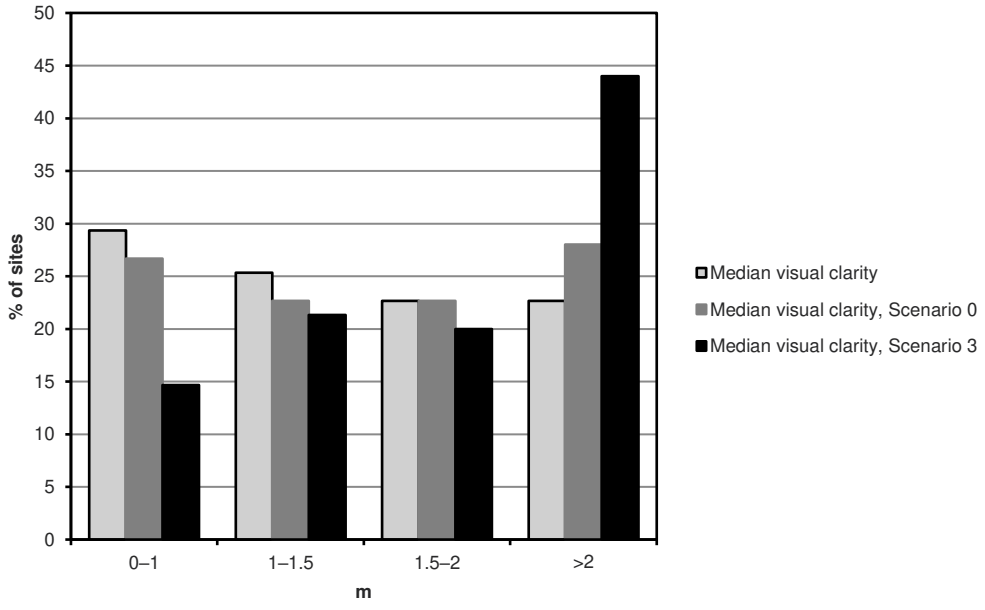

Figure 13. Summary of impact of SLUI by 2043 on median visual clarity (measured in metres) at measurement sites as predicted by scenario 0 and scenario 3.

According to the field data, the average median visual clarity at current monitoring sites is 1.5 m, with 55% of sites having median values below this value (Figure 13). It ranges from 5.0 m at the Waikawa at North Manakau Rd to 0.30 m at the Ohura at the Tokorima site. The impact of SLUI on visual clarity is predicted to be significant, particularly for scenario 3. By 2043 the number of river sites with a median visual clarity of >2 m is predicted to double under scenario 3. Overall, 66 of 124 water management subzones are predicted to have a reduction in SSC by 2043 as a consequence of SLUI, but only 29 of these can be

characterised in terms of visual clarity due to the limited number of measurement sites. These 29 subzones are thus representative of the impact of SLUI in the Horizons region (see Appendix 6, Table 18).

Figure 15 shows the percentage increase in water clarity, which is only found in water management subzones where SLUI works have occurred or are predicted to occur. In Scenario 0, visual clarity is predicted to increase significantly in the Lower Rangitikei (40%), Makuri (36%), and Tamaki–Hopelands (33%) water management subzones. SLUI modelling of scenario 3 has a much greater impact on improving the visual clarity of water, particularly in the Lower Mangawhero (79%), Makuri (72%), Middle Whanganui (71%) and Ōwahanga (65%) water management subzones. For the 29 subzones that are positively affected by SLUI, the average increase in visual clarity is 11% for scenario 0 and 29% for scenario 3. These average increases are possibly representative of the impact on SLUI for the remaining subzones within the SLUI footprint, which do not have associated measurement sites for predicting the relative increase of water clarity.

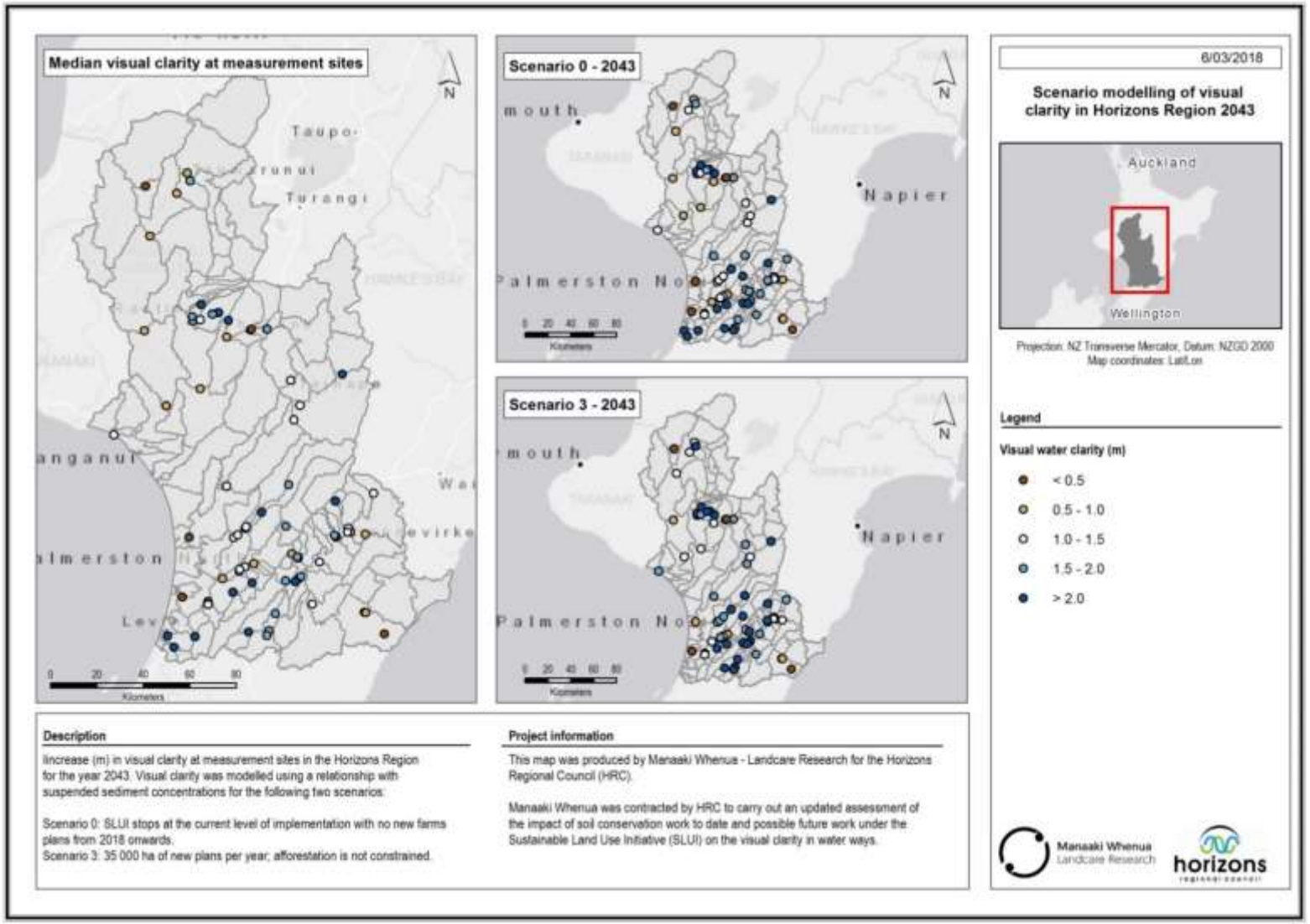

Figure 14. Map showing modelled increase (m) in visual water clarity at measurement sites by 2043.

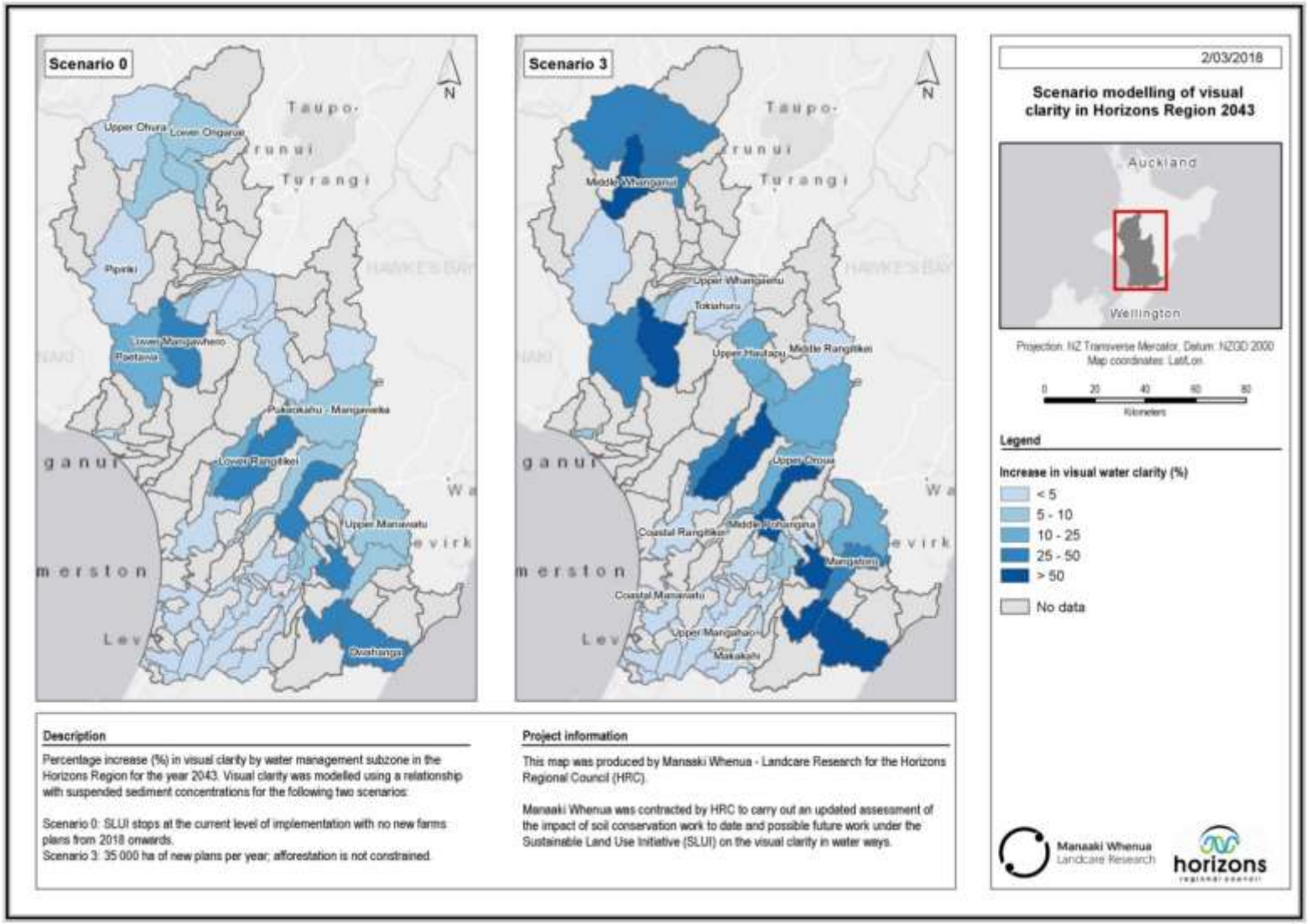

Figure 15. Map showing modelled percentage increase in visual clarity, by water management subzone, at 2043.

9 Conclusions

- SedNetNZ has been used in multiple applications in the Horizons region since 2013. The model algorithms and parameterisation have largely remained the same, with only subtle variations to the sediment delivery ratio and time period of active landsliding.
- The farm-scale version can be used for discussing soil conservation options with farmers but has limited use at the catchment scale because of a lack of whole-catchment or whole erosion terrain farm-scale LUC mapping.
- SedNetNZ typically produces modelled SSY estimates within ±40% of measured SSY, but in some cases there were large overestimates.
- SLUI works to 2017 are estimated to have reduced total regional sediment load by 6%.
- With no further SLUI works it is estimated that by 2043 sediment load for the region will have decreased by 16%. However, with ongoing implementation of SLUI works (scenario 3) sediment load could be decreased by 30%.
- Climate change is predicted to increase sediment yields by 41 to 179% depending on the climate change scenario. To offset these predicted large effects of climate change, continued, and arguably increased, investment in erosion mitigation will be vital.
- SLUI works are predicted to increase mean visual clarity by between 11% (with no further SLUI works) and 29% (scenario 3).

10 Recommendations

- Now that good data are available on the location and area of erosion mitigation works, the analysis of the effect of SLUI erosion control works should be repeated using the area of these works rather than the area of whole farm plans to assess the effect of the difference between whole farm plan area and implemented works area on modelled sediment load reductions from SLUI.
- Better data on the effectiveness of erosion mitigation at whole-farm and whole-catchment scale are needed to test the erosion control effectiveness assumptions derived from hillslope-scale data. Horizons sediment load and farm plan works data could potentially be used for this analysis.
- The farm-scale version of SedNetNZ should not be used at catchment scale because of a lack of whole-catchment or whole-erosion-terrain farm-scale LUC mapping.
- Continued investment in SLUI or other programmes for erosion mitigation will be required to offset the potentially severe effects of climate change.
- The reason(s) why SedNetNZ seriously overestimates sediment load in some catchments is not clear and requires further investigation.
- Current research will result in the replacement of the current surface and bank erosion models in SedNetNZ, and the present analysis should be repeated once these improvements have been made.

11 Acknowledgements

We thank Jon Roygard and Grant Cooper for initiating this work, and Staci Boyte, Willie Mckay, Malcolm Todd and the Horizons data team for providing the SLUI and other data on which this report is based and for discussing the work with us. Ian Lynn, Ray Prebble and Staci Boyte reviewed an earlier draft of this report.

12 References

Alexander RB, Smith RA, Schwarz GE 2004. Estimates of diffuse pollution sources in surface waters of the United States using a spatially referenced watershed model. Water Science and Technology 49: 1–10.

Ausseil A-GE, Dymond JR 2008. Estimating the spatial distribution of sediment concentration in the Manawatu River, New Zealand, under different land-use scenarios. IAHS Publication 325: 502–509.

Betts HD, Basher L, Dymond JR, Herzig A, Marden M, Phillips CJ 2017. Development of a landslide component for a sediment budget model. Environmental Modelling and Software 92: 28–39.

Betts HD, Derose RC 1999. Digital elevation models as a tool for monitoring and measuring gully erosion. International Journal of Applied Earth Observation and Geoinformation 1: 91–101.

Derose RC, Basher LR 2011a. Strategy for the development of a New Zealand SedNet. Landcare Research Contract Report LC226 for AgResearch and Ministry of Science and Innovation.

Derose RC, Basher LR 2011b. Measurement of river bank and cliff erosion from sequential LIDAR and historical aerial photography. Geomorphology 126: 132–147.

Douglas G, Dymond J, McIvor I 2008. Monitoring and reporting of whole farm plans as a tool for affecting land use change. Report for Horizons Regional Council. Palmerston North, AgResearch.

Dymond J 2010. Soil erosion in New Zealand is a net sink of CO_2. Earth Surface Processes and Landforms 35: 1763–1772.

Dymond JR, Betts HD, Schierlitz CS 2010. An erosion model for evaluating regional land-use scenarios. Environmental Modelling and Software 25: 289–298.

Dymond JR, Davies-Colley RJ, Hughes A, Matthaei CD 2017. Predicting improved optical water quality in rivers resulting from soil conservation actions on land. Science of the Total Environment 603−604: 584–592.

Dymond JR, Herzig A, Ausseil A-G 2014. Using SedNetNZ to assess the impact of the Sustainable Land Use Initiative in the Manawatū−Wanganui region on river sediment loads. Landcare Research Contract Report LC1895 for Horizons Regional Council.

Dymond JR, Herzig A, Basher L, Betts HD, Marden M, Phillips CJ, Ausseil A-G, Palmer DJ, Clark M, Roygard J 2016. Development of a New Zealand SedNet model for assessment of catchment-wide soil-conservation works. Geomorphology 257: 85–93.

Dymond J, Herzig A, Betts H, Marden M, Phillips C, Basher L 2013a. Application of SedNetNZ for the assessment of critical source areas in the Manawatu catchment. Landcare Research Contract Report LC1697 for AgResearch and MBIE.

Dymond J, Herzig A, Betts H, Marden M, Phillips C, Basher L 2013b. Parameterisation of SedNetNZ for the Manawatu catchment. Landcare Research Contract Report LC1503 for AgResearch and MBIE.

Dymond J, Manderson A 2015. Updated SedNetNZ estimate according to SLUI 2015 WFP coverage. Letter (Landcare Research Contract Report LC2435) to Horizons Regional Council.

Dymond J, Manderson A 2016. Downscaling sediment yields from 1:50,000 to farm-scale using LUC units. Unpublished report for Horizons Regional Council, Palmerston North, Landcare Research.

Elliott AH, Basher LR 2011. Modelling sediment flux: a review of New Zealand catchment-scale approaches. Journal of Hydrology (NZ) 50: 143–160.

Elliott AH, Shankar U, Hicks DM, Woods RA, Dymond JR 2008. SPARROW regional regression for sediment yields in New Zealand rivers. IAHS Publication 325: 242–249.

Emori S, Taylor K, Hewitson B, Zermoglio F, Juckes M, Lautenschlager M, Stockhause M 2016. CMIP5 data provided at the IPCC Data Distribution Centre. Fact Sheet of the Task Group on Data and Scenario Support for Impact and Climate Analysis (TGICA) of the Intergovernmental Panel on Climate Change (IPCC).

Fahey B, Ekanayake J, Jackson R, Fenemor A, Davie T, Rowe L 2010. Using the WATYIELD water balance model to predict catchment water yields and low flows. Journal of Hydrology (NZ) 49: 35–58.

Fuller IC, Marden M 2010. Rapid channel response to variability in sediment supply: cutting and filling of the Tarndale Fan, Waipaoa catchment, New Zealand. Marine Geology 270: 45–54.

Griffiths GA 1981. Some suspended sediment yields from South Island catchments, New Zealand. Water Resources Bulletin 17: 662–671.

Griffiths GA 1982. Spatial and temporal variability in suspended sediment yields of North Island basins, New Zealand. Journal of the American Water Resources Association 18: 575–584.

Hancox GT, Wright K 2005. Analysis of landsliding caused by the 15–17 February 2004 rainstorm in the Wanganui–Manawatu hill country, southern North Island, New Zealand. Institute of Geological & Nuclear Sciences Science Report 2005/11.

Hawley JG, Dymond JR 1988. How much do trees reduce landsliding? Journal of Soil and Water Conservation 43: 495–498.

Hicks DL 1991. Erosion under pasture, pine plantations, scrub and indigenous forest: a comparison from cyclone Bola. New Zealand Forestry 36: 21–22.

Hicks DL 1995. Control of soil erosion. Ministry of Agriculture Publication 95/4. Wellington, Ministry of Agriculture.

Hicks DM 2011. Review of turbidity and suspended sediment monitoring at Horizons Regional Council. NIWA Client Report CHC2011-021 for Horizons Regional Council.

Hicks DM, Hill J, Shankar U 1996. Variation of suspended sediment yields around New Zealand: the relative importance of rainfall and geology. In: Erosion and Sediment Yield: Global and Regional Perspectives. IAHS Publication No. 236: 149–156.

Hicks DM, Shankar U 2003. Sediment yield from New Zealand rivers. NIWA Chart Miscellaneous Series No. 79. Wellington, NIWA.

Hicks DM, Shankar U, McKerchar AI, Basher L, Jessen M, Lynn I, Page M 2011. Suspended sediment yields from New Zealand rivers. Journal of Hydrology (NZ) 50: 81–142.

Hicks M, Hoyle J 2012. Analysis of suspended sediment yields from the rivers in the Horizons sediment monitoring program. Horizons Report No. 2012/EXT/1284. Palmerston North, Horizons Regional Council.

IPCC 2013. Climate change 2013: the physical science basis. Contribution of Working Group I to the Fifth Assessment Report of the Intergovernmental Panel on Climate Change. Stocker TF, et al. eds. Cambridge, Cambridge University Press, and New York, NY. doi: 10.1017/CBO9781107415324.

Leathwick JR, Morgan F, Wilson G, Rutledge D, McLeod M, Johnston K 2003. Land environments of New Zealand: technical guide. Auckland, David Bateman Ltd.

Manderson A, Douglas G, Mackay A, Dymond J 2011. SLUI Outcomes project: review of the SLUI database and development of a SLUI outcomes reporting framework. Report prepared for Horizons Regional Council by AgResearch.

Manderson A, Dymond J, Ausseil A-G 2015. Climate change impacts on water quality outcomes from the Sustainable Land Use Initiative (SLUI). Landcare Research Contract Report LC2302 for Horizons Regional Council.

Marden M, Betts HD, Arnold G, Hambling R 2008. Gully erosion and sediment load: Waipaoa, Waiapu and Uawa Rivers, eastern North Island, New Zealand. In: Sediment Dynamics in Changing Environments. Proceedings of a symposium held in Christchurch, New Zealand, December 2008. IAHS Publication 325: 339–350.

Marden M, Herzig A, Arnold G 2011. Gully degradation, stabilisation and effectiveness of reforestation in reducing gully-derived sediment, East Coast region, North Island, New Zealand. Journal of Hydrology (NZ) 50: 19–36.

McIvor I, Douglas G, Dymond J, Eyles G, Marden M 2011. Pastoral hillslope erosion in New Zealand and the role of poplar and willow trees in its reduction. In: Soil erosion issues in agriculture. Pp. 257–278. http://www.intechopen.com/articles/show/title/pastoral-hill-slope-erosion-in-new-zealand-and-the-role-of-poplar-and-willow-trees-in-its-reduction.

Ministry for the Environment 2008. Climate change effects and impacts assessment: a guidance manual for local government in New Zealand. 2nd edn. In: Mullan B, Wratt D, Dean S, Hollis M, Allan S, Williams T, Kenny G eds. Wellington, Ministry for the Environment.

Ministry for the Environment 2016. Climate change projections for New Zealand: atmosphere projections based on simulations from the IPCC Fifth Assessment. Wellington, Ministry for the Environment.

Moss RH, Edmonds JA, Hibbard KA, Manning MR, Rose SK, Van Vuuren DP, Carter TR, Emori S, Kainuma M, Kram T, Meehl GA, Mitchell JFB, Nakicenovic N, Riahi K, Smith SJ, Stouffer RJ, Thomson AM, Weyant JP, Wilbanks TJ 2010. The next generation of scenarios for climate change research and assessment. Nature 463: 747–756.

Page M 2008. A bibliography of 'rainfall-induced' landslides in New Zealand. GNS Science Report 2008/08. Wellington, GNS Science.

Page M, Shepherd J, Dymond J, Jessen M 2005. Defining highly erodible land for Horizons Regional Council. Landcare Research Contract Report LC0506/050 for Horizons Regional Council.

Pearce P, Paul V, Mullan B, Zammit C, Sood A, Bell R, Law C 2016. Climate change and variability − Horizons Region. Horizons Report 2016/EXT/1499. Palmerston North, Horizons Regional Council.

Petro S 2013. NZeem® climate change scenarios. Unpublished internal Landcare Research report.

Prosser IP, Young B, Rustomji P, Moran C, Hughes AO 2001. Constructing river basin sediment budgets for the National Land and Water Resources Audit. CSIRO Tech. Rep. 15/01. Canberra, Australia, CSIRO Land and Water.

Reid LM, Page MJ 2003. Magnitude and frequency of landsliding in a large New Zealand catchment. Geomorphology 49: 71–88.

Schierlitz C 2008. New Zealand Empirical Erosion Model (NZeem®): analysis, evaluation and application in climate change scenarios. Unpublished diplomarbeit (thesis), University of Bonn, Germany.

Schierlitz C, Dymond J, Shepherd J 2006. Erosion/sedimentation in the Manawatu catchment associated with scenarios of whole farm plans. Landcare Research Contract Report 0607/028 for Horizons Regional Council.

Thompson RC, Luckman PG 1993. Performance of biological erosion control in New Zealand soft rock hill terrain. Agroforestry Systems 21: 191–211.

Wilkinson S, Henderson A, Chen Y, Sherman B 2004. SedNet user guide: client report. Canberra, CSIRO Land and Water.

Appendix 1 – Original representation of erosion processes in SedNetNZ (after Derose and Basher 2011a)

A1.1 Surface erosion

Dymond (2010) developed a version of the Universal Soil Loss Equation (NZUSLE) to estimate erosion rates from sheet and rill processes. It has the same factors as the USLE except that the rainfall factor is a function of mean annual rainfall only. NZUSLE gives the annual erosion rate ($t \cdot km^{-2} \cdot a^{-1}$) as a product of five factors:

$$HE = \alpha \times P^2 \times K \times LS \times C$$

where: α is a constant (1.2×10^{-3}) calibrated with published surficial erosion rates from New Zealand studies (see Dymond 2010); P is mean annual rainfall (mm); K is the soil erodibility factor (sand 0.05; silt 0.35; clay 0.20; loam 0.25); LS is the slope length factor[14]; C is the vegetation cover factor (bare ground 1.0, pasture 0.01, scrub 0.005, forest 0.005). Derose and Basher (2011a) note that the NZUSLE tends to over-predict rates of erosion despite the very low value for the constant α (Figure 16).

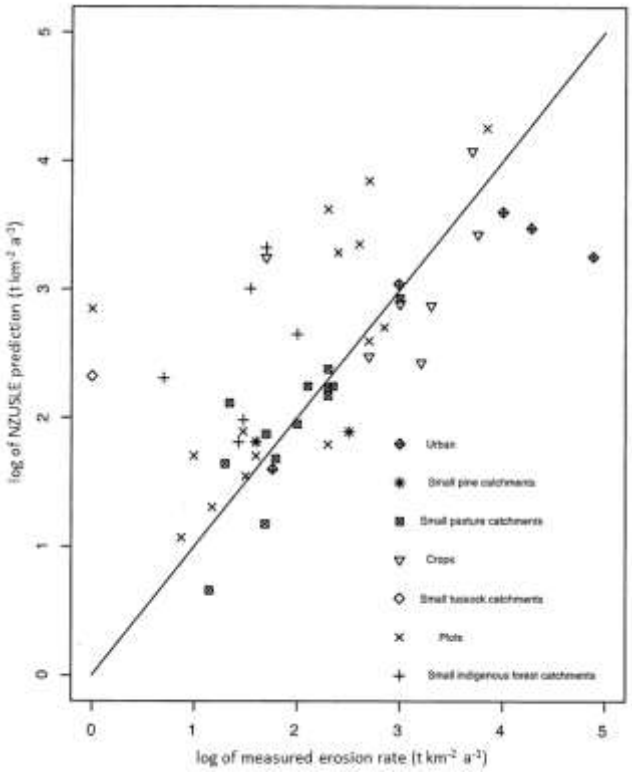

Figure 16. NZUSLE predictions compared to published measurements (from Dymond 2010).

[14] $L = \left(\frac{\lambda}{22}\right)^{0.5}$ where λ = slope length in metres; $S = 0.065 + 4.56\frac{dz}{dx} + 65.41(\frac{dz}{dx})^2$ where $\frac{dz}{dx}$ = slope gradient

A1.2 Shallow landslides

Derose and Basher (2011a) suggested that landslides could be modelled in the same way as gully erosion is modelled in SedNet, with the main input requirement being a probability density grid of the areal extent of hillslopes occupied by landslides (*LD*). The total area of landslides could be calculated as the sum of landslide probability density (values between 0 and 1) for each cell *j* in a catchment (*j* = 1 to n), multiplied by the cell area (*A*, m^2) of the landslide grid. To derive the mass of sediment eroded from hillslopes (*LE*, $t \cdot a^{-1}$), this is multiplied by the average depth of failure below the ground surface (*D*) and soil bulk density (ρ_{ls}), and divided by the period of landslide activity (*T*). Because not all sediment reaches the channel, a sediment delivery ratio (SDR_L) is required to account for losses along the landslide runout path and determine the amount of eroded sediment to reach the stream link. Landslide erosion rates are calculated as:

$$LE = SDR_L \times \frac{\overline{D} \times \rho_{ls} \times A \sum_{j=1}^{n} LD_j}{T}$$

This form of model had not previously been used for landslide modelling, and at the time of the conceptual development of SedNetNZ data was lacking for *LD*, *D*, ρ_{ls} and *SDR*. However, Derose and Basher (2011a) hypothesised that *LD* would vary with slope angle and rock type (Figure 17) and suggested extensive landslide mapping would be required to derive region-wide landslide probability density functions.

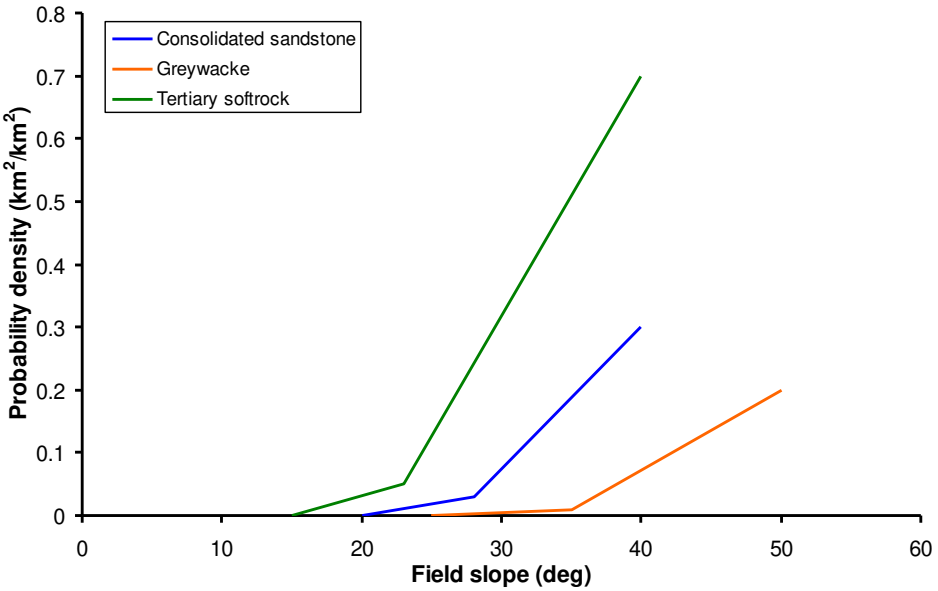

Figure 17. Probability density–slope relationships for landslide-prone grassland hillslopes in North Island hill country over a c. 100-year time period, since forest clearance (from Derose & Basher 2011a)

A1.3 Large landslides

Derose and Basher (2011a) recognised that large landslides could also make a significant contribution to sediment budgets, particularly in extreme rainfall events. For example, during the 2004 storm event in the Manawatu–Rangitikei, large landslides > c. 2,000 m^2,

although representing only about 3% of the number of landslides, accounted for about 48% of the volume of landslide debris eroded from hillslopes (Hancox & Wright 2005). Large landslides also had longer debris tails and were generally connected to the channel more often (higher SDR). Derose and Basher (2011a) suggested that large landslide sediment contribution (*LLE*, t a^{-1}) could be modelled as a function of planform area (A_{LL}), failure depth (D_{LL}), bulk density (ρ_{lls}), SDR and divided by the period of landslide activity (*T*):

$$LLE = SDR_{LL} \times \frac{\rho_{lls} \times \overline{D}_{LL} \times A_{LL}}{T}$$

Derose and Basher (2011a) recognised that although some large landslides are listed in a GNS landslide database, incorporating them in sediment budgets would likely require more mapping.

A1.4 Mass-movement gully complexes

Mass-movement gully complexes, which tend to be large amphitheatre shaped gullies, are the single biggest point-sources of sediment in some New Zealand river basins (e.g. see Marden et al. 2008, 2011, Fuller and Marden 2010) and are characterised by quite different processes to the gullies modelled in SedNet. Derose and Basher (2011a) suggested that sediment generation (*GME*, t a^{-1}) could be modelled as the product of the average sediment delivery ratio (SDR_G), average bulk density of eroding gully materials (ρ_{gs}), and total plan-form area of the actively eroding gullies faces (A_g):

$$GME = SDR_G \times \rho_{gs} \times a \sum_{i=1}^{i=n} A_g^b$$

The constants *a* and *b* depend on the geology within which gullies have formed. In East Coast catchments, Tertiary gullies erode at a constant rate, with *a* = 0.242 and *b* = 1 (Marden et al. 2008). For gullies underlain by crushed Cretaceous lithologies, the denudation rate is proportion to the square root of gully area with *a* = 0.0013 and *b* = 1.5 (Betts and Derose 1999). Modelling mass-movement gully complexes would require maps of individual gully area which are only available for the Gisborne region.

Derose and Basher (2011a) did not include a modelling approach for classic (linear) gully erosion.

A1.5 Tunnel gully erosion

Tunnel gully erosion is a significant process in some areas, particularly where highly permeable layers (e.g. tephra, loess) overlay less permeable soil materials. Derose and Basher (2011a) suggested tunnel gully erosion (*TE*, t·a^{-1}) could be modelled similarly to gully erosion as a function of tunnel gully density (*TD*), average cross-sectional area (α), soil bulk density (ρ_s), sediment delivery ratio, and the period of tunnel gully activity (*T*):

$$TE(t/yr) = SDR_t \times \frac{\alpha \times \rho_s \times A_j \sum_{j=1}^{n} TD_j}{T}$$

Data on tunnel gully density would have to be compiled.

A1.6 Earthflows

Slow-moving earthflows are extensive in some areas of New Zealand and typically deliver sediment directly to stream channels. Derose and Basher (2011a) suggested modelling sediment delivery from earthflows (*EE*) as the product of the average movement rate (M_r, $m \cdot a^{-1}$), cross-sectional area at the toe of the earthflow adjacent to the channel (A_e, m^2) summed for all earthflows, and bulk density of earthflow materials (ρ_{es}):

$$EE = \rho_{es} \times M_r \times \sum_{i=1}^{n} A_{e,i}$$

Earthflows tend to have a restricted range of average depth (c. 5–8 m), so the total cross-sectional area of earthflows intersecting the channel network within a watershed area could be represented by the mean depth (D_e) multiplied by the sum of earthflow widths ($\sum W_e$). The total width in turn could be derived as a proportion of total channel length:

$$A_{e,i} = \overline{D}_e \sum_{i=1}^{i=n} W_{e,i}$$

Derose and Basher (2011a) note that limited data are available for earthflow movement rates and cross-section areas.

A1.7 Bank erosion

Derose and Basher (2011a) reviewed a number of models of bank erosion that incorporated discharge (either bank-full or mean annual), stream power, bank erodibility, bank height, and vegetation cover. They also compiled a data set of bank migration rates for 26 river reaches for New Zealand rivers and found a moderate correlation with WRENZ[15]-modelled mean annual flood discharge (Figure 18) so that bank migration rate (M, $m \cdot a^{-1}$) could be modelled as a function of mean annual flood discharge (Q_{MAF}). The exponent in the regression model was within the range of reported values and slope was not found to be statistically significant in a multiple regression with discharge. They also suggested the effect of riparian vegetation could be incorporated in this model, as a function of the proportion of banks with riparian vegetation (P_r):

$$M = 0.028 * {Q_{MAF}}^{0.469} * (1 - P_r)$$

They also suggested that banks with complete riparian woody cover would erode at one-tenth the rate of banks without any riparian protection.

[15] Water Resources Explorer New Zealand

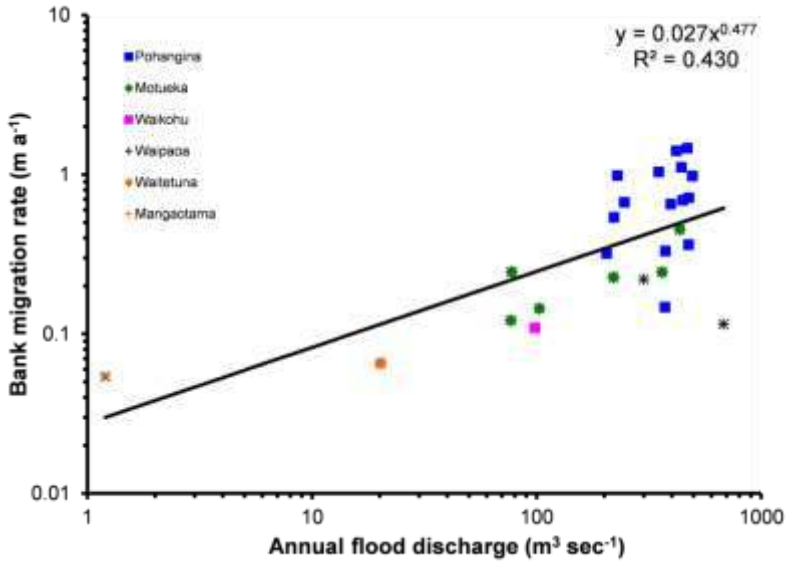

Figure 18. Relationship between average channel migration rate and modelled annual flood discharge for New Zealand rivers.

A1.8 Cliff erosion

Derose and Basher (2011a) suggested cliff erosion (*CLE*) could be modelled as a proportion of the reach having active cliff erosion (P_{cl}), density of bedrock or cliff materials (ρ_{cs}), average cliff height (H_{cl}), length of channel occupied by active cliffs ($P_{cl} \times L_x$), and the average lateral retreat rate of cliffs (M_{cl}):

$$CLE(t/yr) = \rho_{cs} \times \overline{H}_{cl} \times M_{cl} \times (P_{cl} \times L_x)$$

In addition, they suggest that the lateral retreat rate of cliffs (M_{cl}) could be modelled in a similar way to bank erosion (i.e. as a function of discharge or stream power), but required the collection of data on cliff erosion rates. To date only one study has published values of cliff erosion rates (Derose & Basher 2011b), which suggested mean slope angle of cliffs may also need to be included in a cliff erosion model.

A1.9 Deposition

SedNet calculates the proportion of sediment lost to the floodplain from the product of overbank to total discharge for the median flood event and the fraction of sediment that settles out during overbank flow. Derose and Basher (2011a) suggested this has limitations and provided an alternative approach to calculate the proportion of sediment load deposited on floodplains (P_f) from the fraction of sediment that settles out during overbank flow (F_s), the sum of flood sediment concentration (C_{fd}) times overbank discharge ($Q_{ob,i}$), and total sediment load (the sum of concentration (C_d) times daily discharge for all flows ($Q_{d,i}$):

$$P_f = \frac{F_s \times \sum_1^{i=n} C_{fd} \times Q_{\mathrm{ob},i}}{\sum_1^{i=n} C_d \times Q_{\mathrm{d},i}}$$

P_f reduces to the product of three ratios: the mean overbank to mean daily flow-weighted sediment concentration; the average annual overbank to annual total discharge; and the fraction of overbank load that settles out (F_s). Derose and Basher (2011a) suggested the discharge ratio is expected to be c. 0.05 (5%), while the concentration ratio will be >1, and perhaps 2–3.

Appendix 2 – List of erosion terrains for which landslide, gully and earthflow erosion are modelled

Table 12. List of erosion terrains for which landslide, gully and earthflow erosion are modelled

Erosion terrain description	Erosion terrain code	SDR 2013	SDR 2014	Earthflow	Gully
Basins infilled with Taupo tephra flow deposits – intensely gullied	413				
Hill country with loess	611	0.35	0.5		
Hill country with tephra	614	0.35	0.5		
Hill country on mudstone	631	0.35	0.5		
Hill country on crushed mudstone/argillite with moderate earthflow erosion	632	0.35	0.5		
Hill country on crushed mudstone/argillite with severe earthflow erosion	633	0.35	0.5		
Hill country on cohesive sandstone	641	0.35	0.5		
Hill country on non-cohesive sandstone	642	0.35	0.5		
Hill country on limestone	651	0.35	0.5		
Hill country on moderately weathered greywacke/argillite	661	0.35	0.5		
Hill country on slightly weathered white argillite	662	0.35	0.5		
Hilly steeplands on mudstone	731	0.35	0.5		
Hilly steeplands developed on crushed argillite with gully-dominated erosion	732				
Hilly steeplands on sandstone	741	0.35	0.5		
Hilly steeplands on non-cohesive sandstone	742	0.35	0.5		
Hilly steeplands on sandstone/limestone	751	0.35	0.5		
Hilly steeplands on greywacke/argillite	761	0.35	0.5		
Hilly steeplands on white argillite	762	0.35	0.5		
Mountain land on greywacke/argillite/younger sedimentary rocks	911	0.7	0.1		
Mountain land/steepland with sheet/wind/scree erosion	912	0.7	0.1		

Notes: Green boxes indicate earthflow of gully erosion are modelled for these erosion terrains. SDR is for landsliding only. After Dymond et al. (2013b, 2014).

Appendix 3 – Landslide probability density function

Table 13. Landslide probability density function

Slope (°)	% landslide	Slope (°)	% landslide
0	0	22	5.01
1	0.92	23	5.34
2	0	24	5.64
3	1.14	25	5.93
4	0	26	6.71
5	1.33	27	7.5
6	1.35	28	7.55
7	1.38	29	7.6
8	1.52	30	7.91
9	1.66	31	8.23
10	1.9	32	7.91
11	2.14	33	7.59
12	2.26	34	9.29
13	2.38	35	10.99
14	2.53	36	10.36
15	2.68	37	9.73
16	2.96	38	5.59
17	3.24	39	1.46
18	3.74	40	0.11
19	4.25	41	0.8
20	4.47	42	0.4
21	4.69	>42	0

Appendix 4 – SLUI scenario results

Table 14. Scenario 0: sediment loads ($t \cdot a^{-1}$) modelled by SedNetNZ (2004), incorporating SLUI works until 2017, followed by the discontinuation of SLUI with no new farm plans from 2018 onwards. Results are compiled at 5-year intervals from 2013 (SLUI-13) to 2043 (SLUI-43)

Water management zone	2004	SLUI-13	SLUI-18	SLUI-23	SLUI-28	SLUI-33	SLUI-38	SLUI-43	43-04	43-04 %	18-04	18-04 %
Upper Whangaehu	1,438,465	1,438,465	1,437,964	1,437,964	1,437,964	1,437,964	1,437,964	1,437,964	−502	0	−502	0
Middle Rangitikei	1,183,535	1,175,931	1,145,141	1,109,754	1,089,228	1,087,844	1,087,844	1,087,844	−95,691	−8	−38,393	−3
Pipiriki	1,170,999	1,163,567	1,144,856	1,121,513	1,107,819	1,106,657	1,106,657	1,106,657	−64,341	−5	−26,143	−2
Middle Whanganui	1,069,755	1,064,111	1,029,040	989,325	971,406	968,532	968,532	968,532	−101,223	−9	−40,715	−4
Cherry Grove	812,077	808,290	795,328	782,395	774,303	772,562	772,562	772,562	−39,515	−5	−16,749	−2
Lower Whangaehu	774,073	754,322	668,297	576,983	518,779	514,601	514,601	514,601	−259,471	−34	−105,776	−14
Turakina	766,267	741,681	666,782	583,029	546,213	534,932	534,932	534,932	−231,335	−30	−99,485	−13
Oroua	596,940	576,485	536,695	495,022	477,064	471,314	471,314	471,314	−125,626	−21	−60,245	−10
Middle Manawatū	594,941	571,271	517,481	456,029	422,125	412,999	412,999	412,999	−181,942	−31	−77,460	−13
Tiraumea	499,221	494,009	435,884	357,252	300,330	289,321	289,321	289,321	−209,900	−42	−63,336	−13
Lower Rangitikei	497,830	474,506	408,186	343,948	312,598	307,249	307,249	307,249	−190,581	−38	−89,644	−18
Lower Whanganui	361,987	354,333	337,348	316,932	307,235	305,473	305,473	305,473	−56,514	−16	−24,639	−7
Upper Rangitikei	340,503	340,503	339,532	339,532	339,532	339,532	339,532	339,532	−971	0	−971	0
Paetawa	312,293	309,050	290,575	266,859	255,104	254,846	254,846	254,846	−57,447	−18	−21,718	−7
Upper Manawatū	277,501	276,920	269,224	254,045	241,943	238,121	238,121	238,121	−39,381	−14	−8,277	−3
Akitio	275,731	271,513	246,400	217,846	203,590	199,177	199,177	199,177	−76,553	−28	−29,331	−11
Upper Whanganui	264,469	264,549	264,396	264,240	264,232	264,230	264,230	264,230	−239	0	−73	0
Coastal Rangitikei	239,877	239,826	231,443	218,587	207,715	205,644	205,644	205,644	−34,233	−14	−8,434	−4
Ōwahanga	234,063	226,231	202,939	171,446	156,508	153,373	153,373	153,373	−80,690	−34	−31,124	−13
Middle Whangaehu	227,984	227,978	208,806	181,519	158,009	153,468	153,468	153,468	−74,516	−33	−19,178	−8
Mangatainoka	202,165	202,198	199,802	196,395	193,823	193,044	193,044	193,044	−9,120	−5	−2,363	−1

Water management zone	2004	SLUI-13	SLUI-18	SLUI-23	SLUI-28	SLUI-33	SLUI-38	SLUI-43	43-04	43-04 %	18-04	18-04 %
Upper Gorge	201,480	201,184	199,291	197,645	197,297	197,297	197,297	197,297	−4,183	−2	−2,190	−1
Kai Iwi	163,031	152,695	131,990	113,914	107,246	106,172	106,172	106,172	−56,859	−35	−31,042	−19
East Coast	124,984	118,533	101,037	83,531	72,534	70,891	70,891	70,891	−54,093	−43	−23,946	−19
Coastal Manawatū	123,513	123,510	123,510	123,510	123,510	123,510	123,510	123,510	−3	0	−3	0
Manawatū Tamaki Confluence to Hopelands	120,081	117,839	113,665	100,902	90,206	87,145	87,145	87,145	−32,936	−27	−6,416	−5
Lower Manawatū	110,335	110,262	110,097	110,097	110,097	110,097	110,097	110,097	−238	0	−238	0
Coastal Whangaehu	79,445	79,431	79,357	79,283	79,208	79,208	79,208	79,208	−237	0	−88	0
Te Maire	75,506	75,506	74,712	71,345	68,041	65,490	65,490	65,490	−10,016	−13	−795	−1
Northern Coastal	53,007	52,783	51,604	50,425	49,791	49,665	49,665	49,665	−3,343	−6	−1,403	−3
Manawatū Weber Road to Tamaki Confluence	50,403	49,048	48,130	46,232	44,834	44,512	44,512	44,512	−5,892	−12	−2,273	−5
Ohau	43,130	43,130	43,130	43,130	43,130	43,130	43,130	43,130	0	0	0	0
Manawatū Hopelands to Tiraumea Confluence	23,616	23,476	22,742	21,622	20,906	20,906	20,906	20,906	−2,710	−11	−874	−4
Southern Whanganui Lakes	18,887	18,804	18,804	18,804	18,804	18,804	18,804	18,804	−84	0	−84	0
Upper Tamaki	13,888	13,888	13,888	13,888	13,888	13,888	13,888	13,888	0	0	0	0
Waikawa	13,428	13,428	13,428	13,428	13,428	13,428	13,428	13,428	0	0	0	0
Mowhanau	10,729	10,215	9,961	9,789	9,618	9,549	9,549	9,549	−1,179	−11	−768	−7
Northern Manawatū Lakes	9,568	9,554	9,554	9,554	9,554	9,554	9,554	9,554	−14	0	−14	0
Kaitoke Lakes	8,857	8,857	8,857	8,857	8,857	8,857	8,857	8,857	0	0	0	0
Lake Horowhenua	5,380	5,380	5,380	5,380	5,380	5,380	5,380	5,380	0	0	0	0
Upper Kumeti	2,753	2,753	2,753	2,753	2,753	2,753	2,753	2,753	0	0	0	0
Waitarere	2,328	2,328	2,328	2,328	2,328	2,328	2,328	2,328	0	0	0	0
Lake Papaitonga	851	851	851	851	851	851	851	851	0	0	0	0
Total	**13,395,879**	**13,209,195**	**12,561,188**	**11,807,883**	**11,377,781**	**11,294,301**	**11,294,301**	**11,294,301**	**−2,101,578**	**−16**	**−834,691**	**−6**

Table 15. Scenario 3: Sediment loads (t·a^{-1}) modelled by SedNetNZ (2004), incorporating SLUI works until 2017, followed by a continuation of SLUI with 35,000 ha of farm plans implemented from 2018 onwards. Results are compiled at 5-year intervals from 2013 (SLUI-13) to 2043 (SLUI-43)

WMZ_code	2004	SLUI-13	SLUI-18	SLUI-23	SLUI-28	SLUI-33	SLUI-38	SLUI-43	43-04	43-04 %
Upper Whangaehu	1,438,465	1,438,465	1,437,964	1,437,964	1,437,964	1,437,964	1,437,964	1,437,964	−502	0
Middle Rangitikei	1,183,535	1,175,931	1,145,141	1,094,185	1,027,347	979,984	961,123	951,753	−231,781	−20
Pipiriki	1,170,999	1,163,567	1,144,856	1,095,186	1,015,819	943,058	911,815	907,253	−263,745	−23
Middle Whanganui	1,069,755	1,064,111	1,029,040	923,454	758,953	618,508	560,147	550,795	−518,961	−49
Cherry Grove	812,077	808,290	795,328	770,977	731,955	697,562	683,789	679,878	−132,199	−16
Lower Whangaehu	774,073	754,322	668,297	558,711	445,008	377,848	348,734	346,648	−427,425	−55
Turakina	766,267	741,681	666,782	566,392	478,876	408,067	381,456	378,761	−387,506	−51
Oroua	596,940	576,485	536,695	484,785	435,751	394,327	378,556	375,203	−221,738	−37
Middle Manawatū	594,941	571,271	517,481	449,250	389,932	345,355	326,232	323,208	−271,733	−46
Tiraumea	499,221	494,009	435,884	348,628	271,546	239,942	228,526	224,670	−274,551	−55
Lower Rangitikei	497,830	474,506	408,186	337,138	285,932	259,704	250,311	244,631	−253,199	−51
Lower Whanganui	361,987	354,333	337,348	312,244	290,561	273,695	265,475	262,956	−99,031	−27
Upper Rangitikei	340,503	340,503	339,532	339,532	339,532	339,532	339,532	339,532	−971	0
Paetawa	312,293	309,050	290,575	258,440	227,253	209,295	202,608	202,252	−110,041	−35
Upper Manawatū	277,501	276,920	269,224	251,305	226,554	203,560	191,164	185,836	−91,665	−33
Akitio	275,731	271,513	246,400	212,500	181,605	153,471	139,801	136,879	−138,852	−50
Upper Whanganui	264,469	264,549	264,396	264,240	264,232	264,230	264,230	264,230	−239	0
Coastal Rangitikei	239,877	239,826	231,443	214,088	194,259	184,689	180,084	177,605	−62,272	−26
Owahanga	234,063	226,231	202,939	165,466	130,758	107,974	100,566	99,199	−134,863	−58
Middle Whangaehu	227,984	227,978	208,806	173,633	123,651	92,126	85,862	85,812	−142,172	−62
Mangatainoka	202,165	202,198	199,802	196,166	192,753	188,757	186,201	185,588	−16,577	−8
Upper Gorge	201,480	201,184	199,291	197,636	197,214	197,136	197,069	197,041	−4,439	−2
Kai Iwi	163,031	152,695	131,990	113,077	101,332	86,695	75,727	75,183	−87,848	−54

WMZ_code	2004	SLUI-13	SLUI-18	SLUI-23	SLUI-28	SLUI-33	SLUI-38	SLUI-43	43-04	43-04 %
East Coast	124,984	118,533	101,037	80,034	61,985	55,868	54,873	54,249	−70,735	−57
Coastal Manawatū	123,513	123,510	123,510	123,510	123,510	123,510	123,510	123,510	−3	0
Manawatū Tamaki Confluence to Hopelands	120,081	117,839	113,665	98,405	81,669	74,239	72,955	72,405	−47,676	−40
Lower Manawatū	110,335	110,262	110,097	110,097	110,097	110,097	110,097	110,097	−238	0
Coastal Whangaehu	79,445	79,431	79,357	79,282	79,208	79,206	79,206	79,206	−239	0
Te Maire	75,506	75,506	74,712	69,245	60,145	49,699	45,201	43,651	−31,855	−42
Northern Coastal	53,007	52,783	51,604	48,957	42,318	34,638	31,760	31,649	−21,359	−40
Manawatū Weber Road to Tamaki Confluence	50,403	49,048	48,130	45,870	42,917	40,586	39,095	37,740	−12,663	−25
Ohau	43,130	43,130	43,130	43,130	43,130	43,130	43,130	43,130	0	0
Manawatū Hopelands to Tiraumea Confluence	23,616	23,476	22,742	20,464	17,557	16,182	16,074	16,033	−7,583	−32
Southern Whanganui Lakes	18,887	18,804	18,804	18,804	18,804	18,804	18,804	18,804	−84	0
Upper Tamaki	13,888	13,888	13,888	13,888	13,888	13,888	13,888	13,888	0	0
Waikawa	13,428	13,428	13,428	13,428	13,428	13,428	13,428	13,428	0	0
Mowhanau	10,729	10,215	9,961	9,770	9,437	9,221	9,181	9,149	−1,580	−15
Northern Manawatū Lakes	9,568	9,554	9,554	9,554	9,554	9,554	9,554	9,554	−14	0
Kaitoke Lakes	8,857	8,857	8,857	8,857	8,857	8,856	8,856	8,856	−1	0
Lake Horowhenua	5,380	5,380	5,380	5,380	5,380	5,380	5,380	5,380	0	0
Upper Kumeti	2,753	2,753	2,753	2,753	2,753	2,753	2,753	2,753	0	0
Waitarere	2,328	2,328	2,328	2,328	2,328	2,328	2,328	2,328	0	0
Lake Papaitonga	851	851	851	851	851	851	851	851	0	0
Total	**13,395,879**	**13,209,195**	**12,561,188**	**11,569,606**	**10,496,603**	**9,715,696**	**9,397,895**	**9,329,538**	**−4,066,341**	**-30**

Appendix 5 – Assessment of climate change impacts on sediment loads for period 2081–2100: description of methodology:

A5.1 Climate change models

The Coupled Model Inter-comparison Project (CMIP5), a collaborative climate modelling process coordinated by the World Climate Research Programme (WCRP), released a multi-model data set of global coupled ocean-atmosphere general circulation models (Emori et al. 2016). The data set was further analysed by the global scientific community (IPCC Working Group I) to produce the results that underlay the IPCC Fifth Assessment Report (IPCC 2013). Global climate models from the IPCC Fifth Assessment were down-scaled for New Zealand (Ministry for the Environment 2016) to produce detailed regional climate models (RCMs, 5 km grid), which have allowed robust predictions of changes to temperature and precipitation and their spatial and temporal variation to be made. These models were used to analyse and summarise the climate change projections and potential impacts for the Horizons Region by Pearce et al. (2016).

These regional climate models form the basis for modelling the potential impact of climate change on sediment loads for the Horizons region. Four scenarios, or representative concentration pathways (RCPs), are used to characterise a variety of trends depending on the approximate radiative forcing at 2100 relative to 1750:

- 2.6 $W \cdot m^{-2}$ for RCP2.6
- 4.5 W·m-2 for RCP4.5
- 6.0 $W \cdot m^{-2}$ for RCP6.0
- 8.5 $W \cdot m^{-2}$ for RCP8.5.

These scenarios are based on different decisions related to the socio-economic developments and land-use changes through the century that influence the future concentrations of greenhouse gases and aerosols in the atmosphere.

The first of these RCPs is a mitigation pathway (RCP2.6), which would see a reduction of CO2 concentration in the atmosphere; RCP4.5 and RCP6.0 are both 'stabilisation pathways', where concentration levels gradually steady, though at higher levels than today. RCP8.5 is what is referred to as a 'business as usual' pathway, where CO2 concentrations steadily increase throughout the century. RCPs 4.5 and 8.5 correspond fairly well to the B1 and A1 1FI, respectively, of the Fourth Assessment Report (see Figure 19). We used regional climate models for six general circulation models:

- BCC-CSM1.1
- CESM1-CAM5
- GFDL-CM3
- GISS-E2-R
- HadGEM2-ES
- NorESM1-M.

These six GCMs were dynamically down-scaled to produce projections for a large number of weather variables and were selected based on the validation results in the New Zealand region in their historical simulations (see Ministry for the Environment 2016 for details on methodology).

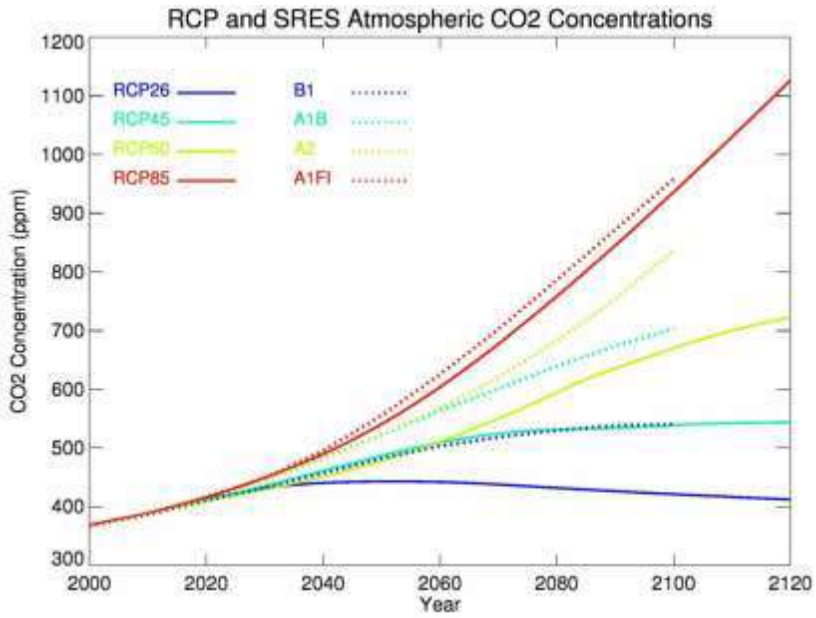

Figure 19. Atmospheric carbon dioxide concentrations for the IPCC Fourth Assessment (dotted lines, SRES concentrations) and for the IPCC Fifth Assessment (solid lines, RCP concentrations); Source: Ministry for the Environment 2016.

The previous report on modelling the impact of climate change on erosion rates and sediment loads for the Horizons Region (Manderson et al. 2015) did so using the A1B (moderate impact), A1FI (fossil-fuel intensive representing at major impact), and a third 'minor impact' scenario, which was defined as a half-way point between the status quo and A1B. Manderson et al. (2015) made predictions based on the IPCC time period 2030−2049. This report complements the previous analysis by extending the horizon to assess the potential impact of climate change on sediment loads for the period 2081−2100, which is abbreviated as 2090.

A5.2 Dominant erosion processes in hill country and lowland areas

Schierlitz (2008) investigated the potential impact of climate change on future sediment loads in the Manawatū catchment using the NZeem model (Dymond et al. 2010). Two different methods were used for this assessment based on changes to mean annual precipitation and storminess. The first method using mean annual precipitation showed changes in annual precipitation to be modest and variable (−2.7% to 3.1% at sub-catchment scale), leading Schierlitz (2008) to conclude that changes in mean annual rainfall will not dramatically affect mean erosion rates or sediment yields (i.e. rainfall alone is inadequate). Increased storminess on the other hand, resulted in a notable sediment loss across all catchments, and a net 52% increase across the whole catchment. The storminess method also produced lower levels of error.

Therefore we use two different models to characterise the impact of climate change by distinguishing between the dominant erosion processes in hill country and lowland areas. Shallow landsliding is the dominant erosion process in hill country in the Horizons region, whereas surficial erosion is the more dominant process in lowland areas. Each of these processes has a different driver of change. The rate of landslide erosion is a function of frequency (return interval) and magnitude (landslide density). Therefore the change in storminess, i.e. the frequency of storms is the method used to assess the impact of climate change in hill country.

Estimating impact of climate change on landslide erosion

Daily rainfall data from meteorological sites from around New Zealand were obtained from the CliFlo database (https://cliflo.niwa.co.nz/) and analysed for continuity and completeness. Data sets with a complete record history of more than 75 years were selected, and an exercise was undertaken to representatively match a core set of meteorological sites to Land Environments New Zealand (LENZ; Leathwick et al. 2003). LENZ is a spatial database that integrates climate variability across New Zealand, and is used here as a proxy to help distribute the point data sets.

Rainfall records for a final 50 meteorological sites were analysed using a Python script, which isolated storm rainfall according to the definition of Reid and Page (2003, p. 76); i.e. 'the sum of daily rainfalls during a period bounded by days with less than 10 mm of rain'. These data sets represent a historical record of storms and their magnitude throughout New Zealand for the past 75 years. They are used here as a baseline to evaluate the impact of climate change projections on erosion and sediment yields.

Following the method adopted by Manderson et al. (2015), historical rainfall records covering the past 75 years are analysed to quantify the frequency and magnitude of future storms given the projected increase in average annual temperature. As temperature increases, the atmosphere's capacity to hold larger quantities of water increases, which is likely to result in more frequent heavy rainfall events. The Ministry for the Environment (2008) provide percentage adjustments for estimating the change in heavy rainfall per 1°C temperature increase due to climate change. The percentage adjustments range from 3.5% for an average recurrence interval (ARI) of 2 years and a duration of 72 hours, up to 8% for all storm durations with an ARI of 50 and 100 years. We use the augmentation factor of 7.8%, which is the value used to represent a rainfall event with an ARI of 30 years and duration of 48 hours. Such an event currently corresponds to a rainfall depth of 119 mm, based on rainfall depth-duration-frequency statistics for Palmerston North from the High Intensity Rainfall Design System (HIRDS v3) (Pearce et al. 2016). Depending on the cumulative rainfall and corresponding soil moisture levels, landslide-triggering rainfall events generally require a minimum storm rainfall of 125−200 mm (Reid & Page 2003). We therefore use a value of 7.8% to approximate future storm rainfall (R') per 1°C increase in average annual temperature (ΔT) based on historical records of rainfall (R) from meteorological sites:

$$R' = R + (\Delta T \times 1.078 \times R) \quad (1)$$

Equation 1 was applied to each storm rainfall data set, using the ΔT from the six models and four IPCC RCP scenarios for the period 2081−2100 (or 2090). Using the historical data

sets, we assume the same frequency distribution of storms in the future. Figure 20 is sourced from Pearce et al. (2016) and shows the projected seasonal temperature in 2090 for the RCP 8.5 scenario, suggesting that temperatures may increase by up to 3–3.5°C through most of the year.

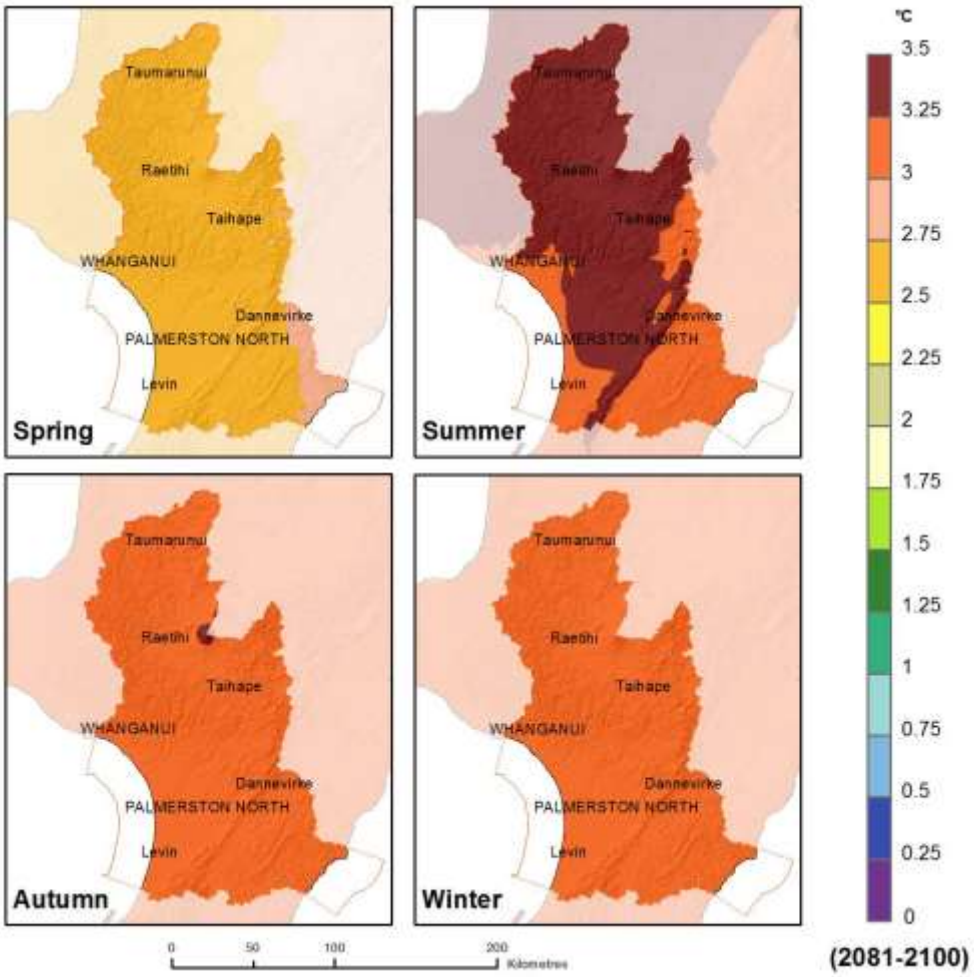

Figure 20. Projected seasonal temperature changes at 2090 (2081–2100 average), relative to 1986–2005 average, for the IPCC RCP 8.5 scenario, averaged over 41 climate models. ©NIWA. Source: Pearce et al. 2016.

Relating landslide density to storm rainfall magnitude

Reid and Page (2003) measured a temporal sequence of landslides in an East Coast catchment and correlated landslide density (number per square kilometre) with storm magnitude (Figure 21). They concluded that landslides directly contributed 15 ±5% of the suspended sediment load in the catchment's river, and that 75% of the sediment production from landslides had occurred during storms with a recurrence interval less than 27 years.

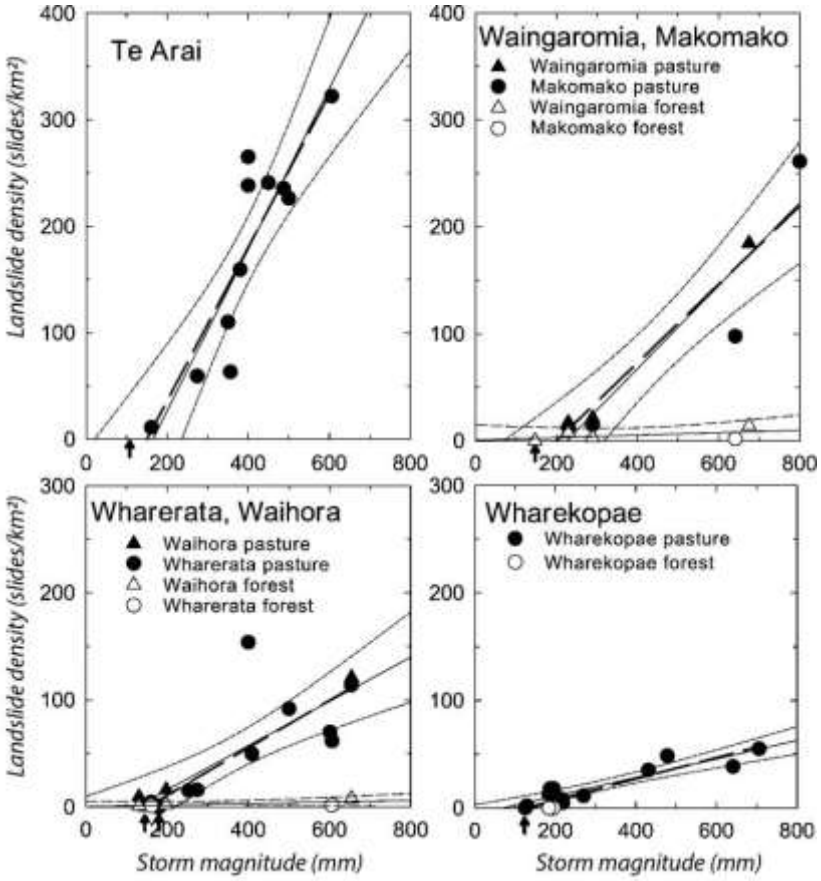

Figure 21. Relationship between landslide density and storminess by six land types within the Waipaoa catchment (from Reid & Page 2003). Arrows on the horizontal axes indicate the storm rainfall thresholds that triggered erosion (with 150 mm being a representative value).

Reid and Page (2003) found a linear relationship between landslide density and storm rainfall (Figure 21). The relationships differed between the land systems with varying rainfall thresholds for triggering landslides. The Te Arai land system is characterised by the highest proportion of pastoral land, so it was used as a proxy for generating landslide density from storm magnitude, using the 150 mm threshold that was used to fit the regression:

$$LD = 0.72R - 108 \quad (2)$$

where LD is the landslide density, and R the storm rainfall in mm.

For each of the four IPCC RCP scenarios and six regional climate models (RCMs), the landslide density was calculated based on the rainfall magnitudes calculated using equation (1), and linear equations were fitted. These equations were assigned to LENZ environments and a multiplier coefficient for change (100 m pixel scale) in landslide erosion due to ΔT was assigned.

The factor of change calculated using this method is applied to assess change to erosion on hillslopes, where landsliding is the dominant erosion process. However, we expect that as the frequency and intensity of rainfall events increase due to climate change, the rates of other forms of mass movement and fluvial erosion processes on hillslopes will become

increasingly active as well. Therefore, the same factor of change is used as a proxy for all hillslope erosion processes and applied to earthflow, gully and surficial erosion, accordingly. SedNetNZ is used to model the four hillslope erosion processes of landslide, earthflow, gully and surficial erosion. The erosion modelling results are aggregated to a single raster layer (15 m pixel scale) and multiplied by the factors of change for each IPCC RCP scenario and RCM.

Estimating impact of climate change on surficial erosion

The main driver of change to surficial erosion is precipitation, as both the NZeem and the NZUSLE models (see Dymond et al. 2016) assume a power law relationship with rainfall; i.e. $\bar{e}(x, y) \propto R^2(x, y)$; thus a 10% change in rainfall would result in a 20% change in erosion. LENZ (Leathwick et al. 2003) is used to differentiate between hill country and lowland areas. Again, the impact of changing precipitation was assessed for each of the four IPCC RCP scenarios and six RCMs using the NZUSLE model (surficial erosion component of SedNetNZ). The resulting outputs are factors of change for lowland areas, where surficial erosion is assumed to be the dominant process. As with the factors of change for hill country, these factors were multiplied by the aggregated output of SedNetNZ hillslope sediment yield (15 m pixel scale).

Figure 22 shows the projected seasonal precipitation changes at 2090 for the IPCC RCP 8.5 scenario. The projected changes indicate a slight increase in rainfall during summer months in the eastern part of the Horizons region (5−15%), but a general decrease in winter east of the Ruahine Ranges in winter (up to 20% less rainfall). In contrast, winters in the hill country west of the ranges are expected to become drier. However, for other seasons, the projected precipitation change remains ±5%.

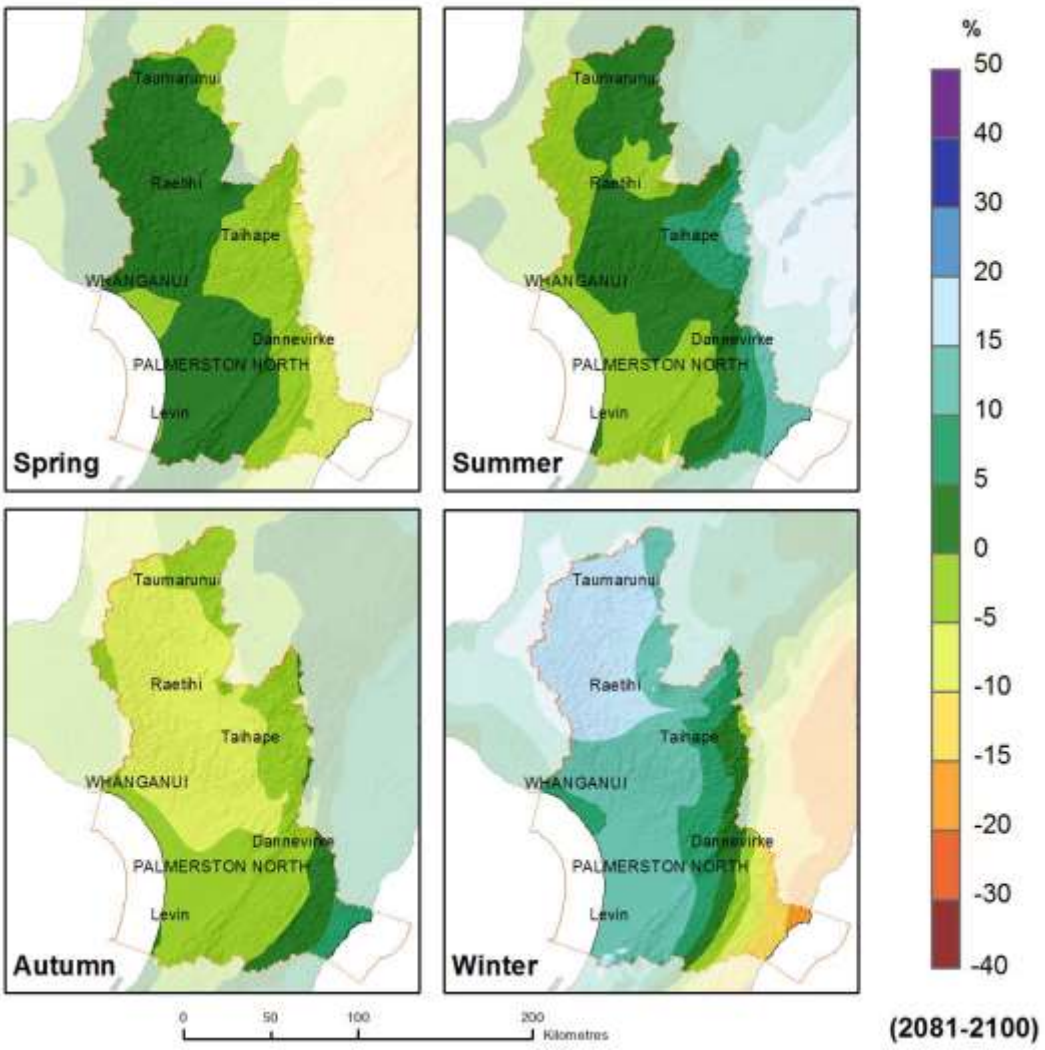

Figure 22. Projected seasonal precipitation changes (in %) at 2090 (2081−2100 average), relative to 1986−2005 average, for the IPCC RCP 8.5 scenario, averaged over 41 climate models. ©NIWA. Source: Pearce et al. (2016).

Table 16. Results of analysis of climate change impacts on sediment loads

Water management zone	SedNetNZ sediment load baseline[a]	AVG RCP.2.6 sediment load	AVG RCP 4.5 sediment load	AVG RCP 6.0 sediment load	AVG RCP 8.5 sediment load	AVG RCP 2.6 change %	AVG RCP 4.5 change %	AVG RCP 6.0 change %	AVG RCP 8.5 change %
Akitio	253,002	410,581	569,111	694,553	936,953	62	125	175	270
Cherry Grove	720,697	1,066,486	1,402,662	1,680,585	2,238,718	48	95	133	211
Coastal Manawatū	41,669	60,712	81,018	97,402	127,047	46	94	134	205
Coastal Rangitikei	178,666	267,337	355,244	427,272	562,730	50	99	139	215
Coastal Whangaehu	35,067	40,195	45,556	49,748	57,849	15	30	42	65
East Coast	125,532	197,985	268,209	323,498	432,311	58	114	158	244
Kai Iwi	166,904	246,901	325,841	388,363	509,450	48	95	133	205
Kaitoke Lakes	4,550	3,852	2,985	2,319	1,163	−15	−34	−49	−74
Lake Horowhenua	1,577	2,371	3,263	3,980	5,331	50	107	152	238
Lake Papaitonga	62	63	64	63	66	2	3	2	7
Lower Manawatū	66,650	76,572	85,804	93,319	107,437	15	29	40	61
Lower Rangitikei	452,878	572,003	689,330	783,142	968,257	26	52	73	114
Lower Whangaehu	717,108	1,171,829	1,633,090	1,997,251	2,697,127	63	128	179	276
Lower Whanganui	310,460	414,243	521,272	605,258	766,413	33	68	95	147
Manawatū Hopelands to Tiraumea Confluence	21,074	34,181	47,844	58,493	78,832	62	127	178	274
Manawatū Tamaki Confluence to Hopelands	102,216	162,618	226,722	276,075	373,105	59	122	170	265
Manawatū Weber Road to Tamaki Confluence	43,880	59,955	77,174	90,698	117,386	37	76	107	168
Mangatainoka	138,629	209,036	284,069	342,819	451,943	51	105	147	226
Middle Manawatū	575,650	922,940	1,268,003	1,544,970	2,081,528	60	120	168	262
Middle Rangitikei	1,081,489	1,597,222	2,105,676	2,506,519	3,334,350	48	95	132	208
Middle Whangaehu	219,821	370,458	527,272	650,287	896,726	69	140	196	308
Middle Whanganui	1,013,240	1,722,492	2,474,476	3,076,481	4,251,142	70	144	204	320

Water management zone	SedNetNZ sediment load baseline[a]	AVG RCP.2.6 sediment load	AVG RCP 4.5 sediment load	AVG RCP 6.0 sediment load	AVG RCP 8.5 sediment load	AVG RCP 2.6 change %	AVG RCP 4.5 change %	AVG RCP 6.0 change %	AVG RCP 8.5 change %
Mowhanau	6,226	5,909	5,302	4,918	4,221	−5	−15	−21	−32
Northern Coastal	44,537	67,217	89,521	107,219	141,402	51	101	141	217
Northern Manawatū Lakes	76	84	86	87	93	11	13	14	22
Ohau	34,302	48,468	63,035	74,828	96,731	41	84	118	182
Oroua	565,130	817,165	1,057,353	1,250,382	1,629,583	45	87	121	188
Owahanga	222,397	350,783	480,357	583,873	782,050	58	116	163	252
Paetawa	259,377	439,909	626,808	774,543	1,052,253	70	142	199	306
Pipiriki	1,017,706	1,706,182	2,433,526	3,000,824	4,095,551	68	139	195	302
Southern Whanganui Lakes	707	396	39	−239	−743	−44	−94	−134	−205
Te Maire	62,413	105,063	149,035	184,778	255,406	68	139	196	309
Tiraumea	520,270	858,770	1,215,562	1,497,261	2,022,636	65	134	188	289
Turakina	741,721	1,137,230	1,546,465	1,870,804	2,508,076	53	108	152	238
Upper Gorge	166,958	221,547	276,829	320,655	402,633	33	66	92	141
Upper Kumeti	2,163	3,033	3,943	4,648	6,066	40	82	115	180
Upper Manawatū	256,029	391,418	529,319	640,229	848,689	53	107	150	231
Upper Rangitikei	316,884	394,407	468,231	526,541	647,531	24	48	66	104
Upper Tamaki	12,488	20,211	28,365	34,599	47,484	62	127	177	280
Upper Whangaehu	1,490,214	2,228,600	2,592,757	2,891,317	3,498,070	50	74	94	135
Upper Whanganui	236,003	319,187	397,890	463,199	598,468	35	69	96	154
Waikawa	10,831	14,925	19,230	22,727	29,478	38	78	110	172
Waitarere	56	58	59	60	65	3	6	7	16
Total	**12,237,309**	**18,740,597**	**24,978,398**	**29,946,353**	**39,661,609**	**41**	**82**	**115**	**179**

[a] Only hillslope erosion processes (landslide, earthflow, gully and surficial erosion) are included in the modelled baseline. These figures correspond to Appendix 4, but differ in that the sediment loads in Appendix 4 account for river bank erosion.

Appendix 6 – Visual clarity results

Table 17. Median visual clarity (*v*, m) and relationship with suspended sediment concentration (SSC) for measurement sites. WMSZ = associated water management subzone. See section 4.4 for a description of method of determining the constants *d* and *c*

Measurement site	WMSZ	Zone code	Median *v* (m)	Intercept *d*	Gradient *c*	r^2
Hautapu at Alabasters	Upper Hautapu	Rang_2f	1.20	1.165	−0.561	0.533
Hautapu at u/s Rangitikei River Conf	Lower Hautapu	Rang_2g	1.02	1.100	−0.542	0.685
Kahuterawa at Johnstons Rata	Kahuterawa	Mana_11c	2.02	1.344	−0.632	0.363
Makakahi at d/s Eketahuna STP	Makakahi	Mana_8d	1.95	1.032	−0.527	0.576
Makakahi at Hamua	Makakahi	Mana_8d	1.65	0.938	−0.455	0.341
Makakahi at u/s Eketahuna STP	Makakahi	Mana_8d	2.00	1.010	−0.410	0.340
Makotuku at d/s Raetihi STP	Lower Makotuku	Whau_3c	1.70	0.956	-0.424	0.242
Makotuku at Raetihi	Lower Makotuku	Whau_3c	2.00	1.228	-0.575	0.422
Makotuku at SH49A	Upper Makotuku	Whau_3b	3.00	1.538	−0.576	0.423
Makuri at Tuscan Hills	Makuri	Mana_7d	1.15	1.224	−0.657	0.734
Manawatū at ds Fonterra Longburn	Lower Manawatū	Mana_11a	1.20	1.032	−0.504	0.483
Manawatū at Hopelands	Tamaki – Hopelands	Mana_5a	1.20	1.279	−0.640	0.777
Manawatū at Opiki Br	Lower Manawatū	Mana_11a	0.74	1.538	−0.739	0.750
Manawatū at Teachers College	Middle Manawatū	Mana_10a	0.73	0.913	−0.536	0.700
Manawatū at u/s PNCC STP	Lower Manawatū	Mana_11a	1.05	1.134	−0.590	0.621
Manawatū at u/s PPCS Shannon	Coastal Manawatū	Mana_13a	0.50	0.390	−0.366	0.261
Manawatū at Upper Gorge	Upper Gorge	Mana_9a	0.95	1.351	−0.643	0.792
Manawatū at us Fonterra Longburn	Lower Manawatū	Mana_11a	1.37	0.929	−0.435	0.442
Manawatū at Weber Road	Upper Manawatū	Mana_1a	0.95	1.158	−0.656	0.793

Measurement site	WMSZ	Zone code	Median *v* (m)	Intercept *d*	Gradient *c*	r^2
Manawatū at Whirokino	Coastal Manawatū	Mana_13a	0.38	0.726	−0.527	0.459
Mangaatua at d/s Woodville STP	Mangaatua	Mana_9c	1.40	0.925	−0.401	0.341
Mangaatua at u/s Woodville STP	Mangaatua	Mana_9c	1.60	1.220	−0.623	0.678
Mangaehuehu at d/s Rangataua STP	Tokiahuru	Whau_1c	2.18	1.182	−0.414	0.365
Mangaehuehu at u/s Rangataua STP	Tokiahuru	Whau_1c	2.60	1.311	−0.423	0.314
Mangahao at Ballance	Upper Mangahao	Mana_9d	2.00	1.248	−0.607	0.631
Mangaore at d/s Shannon STP	Mangaore	Mana_13d	1.00	1.120	−0.653	0.613
Mangaore at u/s Shannon STP	Mangaore	Mana_13d	1.02	1.022	−0.640	0.631
Mangapapa at Troup Rd	Mangapapa	Mana_9b	1.75	1.181	−0.665	0.481
Mangarangiora trib at ds Norsewood STP	Upper Manawatū	Mana_1a	1.40	0.772	−0.355	0.135
Mangarangiora Trib at US Norsewood STP	Upper Manawatū	Mana_1a	1.50	0.599	−0.182	0.056
Mangatainoka at Brewery − S.H.2 Bridge	Lower Mangatainoka	Mana_8c	2.20	1.233	−0.557	0.636
Mangatainoka at d/s DB Breweries	Lower Mangatainoka	Mana_8c	1.95	1.106	−0.513	0.410
Mangatainoka at d/s Pahiatua STP	Lower Mangatainoka	Mana_8c	2.31	1.054	−0.281	0.185
Mangatainoka at Larsons Road	Upper Mangatainoka	Mana_8a	3.00	1.432	−0.581	0.406
Mangatainoka at u/s Pahiatua STP	Lower Mangatainoka	Mana_8c	2.50	1.198	−0.506	0.378
Mangatera at Dannevirke	Mangatera	Mana_2b	1.39	1.221	−0.541	0.603
Mangatera at u/s Manawatū confluence	Mangatera	Mana_2b	1.02	1.292	−0.618	0.756
Mangatoro at Mangahei Road	Mangatoro	Mana_1c	0.82	1.341	−0.664	0.595
Mangawhero at d/s Ohakune STP	Upper Mangawhero	Whau_3d	1.60	0.936	−0.465	0.326
Mangawhero at DOC Headquarters	Upper Mangawhero	Whau_3d	3.00	1.412	−0.463	0.367
Mangawhero at Pakihi Rd Bridge	Upper Mangawhero	Whau_3d	1.42	0.756	−0.463	0.338

Measurement site	WMSZ	Zone code	Median *v* (m)	Intercept *d*	Gradient *c*	r^2
Mangawhero at Raupiu Road	Lower Mangawhero	Whau_3e	0.75	0.831	−0.630	0.715
Mangawhero at u/s Ohakune STP	Upper Mangawhero	Whau_3d	1.71	1.011	−0.491	0.381
Mowhanau Stream at Footbridge	Mowhanau Estuary	West_3CMA	1.17	1.281	−0.585	0.383
Ohau at Gladstone Reserve	Upper Ohau	Ohau_1a	4.93	1.775	−0.525	0.392
Ohau at Haines Property	Lower Ohau	Ohau_1b	3.55	1.718	−0.686	0.578
Ohura at Tokorima	Upper Ohura	Whai_4b	0.30	0.302	−0.439	0.454
Ongarue at Taringamotu	Lower Ongarue	Whai_2g	0.90	1.198	−0.603	0.608
Oroua at Almadale Slackline	Upper Oroua	Mana_12a	2.20	1.737	−0.688	0.856
Oroua at Awahuri Bridge	Middle Oroua	Mana_12b	1.09	1.345	−0.609	0.786
Oroua at d/s AFFCO Feilding	Middle Oroua	Mana_12b	1.50	1.406	−0.665	0.814
Oroua at d/s Feilding STP	Middle Oroua	Mana_12b	1.28	1.409	−0.604	0.768
Oroua at U/S AFFCO Feilding	Middle Oroua	Mana_12b	1.40	1.358	−0.622	0.803
Oroua at U/S Feilding STP	Middle Oroua	Mana_12b	1.50	1.397	−0.593	0.777
Oroua Trib at U/S Kimbolton STP	Upper Oroua	Mana_12a	1.88	0.922	−0.374	0.278
Oroua tributary at d/s Kimbolton STP	Upper Oroua	Mana_12a	1.50	1.046	−0.417	0.253
Oruakeretaki at d/s PPCS Oringi STP	Oruakeretaki	Mana_5d	2.11	1.243	−0.501	0.465
Oruakeretaki at S.H.2 Napier	Oruakeretaki	Mana_5d	1.95	1.409	−0.631	0.490
Owahanga at Branscombe Bridge	Owahanga	Owha_1	0.35	0.721	−0.585	0.754
Pohangina at Mais Reach	Middle Pohangina	Mana_10c	1.60	1.528	−0.647	0.686
Pongaroa at d/s Pongaroa STP	Owahanga	Owha_1	0.50	0.812	−0.631	0.793
Pongaroa at u/s Pongaroa STP	Owahanga	Owha_1	0.55	0.708	−0.612	0.808
Porewa at d/s Hunterville STP	Porewa	Rang_4c	0.70	1.198	−0.652	0.672

Measurement site	WMSZ	Zone code	Median *v* (m)	Intercept *d*	Gradient *c*	r^2
Porewa at d/s Hunterville STP site A	Porewa	Rang_4c	0.58	0.683	−0.804	0.589
Porewa at u/s Hunterville STP	Porewa	Rang_4c	1.10	0.930	−0.498	0.554
Porewa at u/s Hunterville STP site A	Porewa	Rang_4c	0.60	0.669	−0.890	0.639
Rangitikei at Mangaweka	Pukeokahu − Mangaweka	Rang_2b	1.20	1.320	−0.639	0.760
Rangitikei at McKelvies	Coastal Rangitikei	Rang_4a	0.50	1.825	−0.722	0.794
Rangitikei at Onepuhi	Lower Rangitikei	Rang_3a	1.35	1.896	−0.751	0.808
Rangitikei at Pukeokahu	Middle Rangitikei	Rang_2a	3.20	1.581	−0.668	0.615
Tamaki at Tamaki Reserve	Upper Tamaki	Mana_3	2.75	1.410	−0.584	0.654
Tokiahuru at Junction	Tokiahuru	Whau_1c	0.90	0.813	−0.586	0.408
Tokomaru River at Horseshoe bend	Upper Tokomaru	Mana_13b	2.91	1.299	−0.410	0.205
Waikawa at North Manakau Road	Waikawa	West_9a	5.00	1.792	−0.476	0.316
Waikawa Stream at Huritini	Waikawa	West_9a	0.80	1.282	−0.682	0.570
Waitangi at d/s Waiouru STP	Waitangi	Whau_1b	1.53	0.929	−0.294	0.213
Waitangi at u/s Waiouru STP	Waitangi	Whau_1b	1.55	1.104	−0.381	0.295
Whangaehu at d/s Winstone Pulp	Upper Whangaehu	Whau_1a	0.30	0.513	−0.478	0.277
Whangaehu at u/s Winstone Pulp	Upper Whangaehu	Whau_1a	0.37	0.782	−0.523	0.393
Whanganui at Cherry Grove	Cherry Grove	Whai_2a	1.60	1.382	−0.643	0.634
Whanganui at Pipiriki	Pipiriki	Whai_5a	0.60	1.106	−0.603	0.741
Whanganui at Te Maire	Te Maire	Whai_3	1.00	1.142	−0.587	0.694
Whanganui at Te Rewa	Paetawa	Whai_6	0.78	0.993	−0.568	0.618
Whanganui at Wades Landing	Middle Whanganui	Whai_4a	0.77	1.199	−0.658	0.767

Table 18. Impact of SLUI on visual clarity (*v*, m) for water management subzones associated with measurement sites and percentage increases. S0 2043 = scenario 0, 2043; S3 2043 = scenario 3, 2043. Only water management subzones impacted by SLUI farm plans are listed.

WMSZ	Zone code	Water management zone	Median *v* (m) AT ASSOCIATED SITE	Median *v* (m) S0 2043	Median *v* (m) S3 2043	% increase S0 2043	% increase S3 2043
Lower Mangawhero	Whau_3e	Lower Whangaehu	0.75	0.95	1.34	26.23	78.64
Makuri	Mana_7d	Tiraumea	1.15	1.57	1.97	36.15	71.65
Middle Whanganui	Whai_4a	Middle Whanganui	0.77	0.81	1.31	6.43	71.30
Owahanga	Owha_1	Owahanga	0.47	0.59	0.77	26.68	65.20
Tamaki – Hopelands	Mana_5a	Manawatu Tamaki Confluence to Hopelands	1.20	1.60	1.96	33.15	63.00
Lower Rangitikei	Rang_3a	Lower Rangitikei	1.35	1.90	2.16	40.48	60.02
Middle Pohangina	Mana_10c	Middle Manawatū	1.60	2.07	2.48	29.28	55.25
Cherry Grove	Whai_2a	Cherry Grove	1.60	1.74	2.36	8.74	47.58
Porewa	Rang_4c	Coastal Rangitikei	0.75	0.88	1.05	18.05	40.53
Te Maire	Whai_3	Te Maire	1.00	1.08	1.37	8.76	38.17
Mangatoro	Mana_1c	Upper Manawatū	0.82	0.89	1.10	9.30	34.43
Lower Ongarue	Whai_2g	Cherry Grove	0.90	0.95	1.21	5.64	34.31
Upper Ohura	Whai_4b	Middle Whanganui	0.30	0.30	0.39	0.11	30.39
Paetawa	Whai_6	Paetawa	0.78	0.87	0.99	11.62	27.34
Lower Hautapu	Rang_2g	Middle Rangitikei	1.02	1.05	1.22	3.80	20.51
Upper Manawatū	Mana_1a	Upper Manawatū	1.28	1.38	1.52	8.04	18.76
Upper Oroua	Mana_12a	Oroua	1.86	1.97	2.17	5.85	16.73
Pukeokahu – Mangaweka	Rang_2b	Middle Rangitikei	1.20	1.28	1.40	7.03	16.37

WMSZ	Zone code	Water management zone	Median v (m) AT ASSOCIATED SITE	Median v (m) S0 2043	Median v (m) S3 2043	% increase S0 2043	% increase S3 2043
Upper Hautapu	Rang_2f	Middle Rangitikei	1.20	1.22	1.36	1.70	13.64
Mangapapa	Mana_9b	Upper Gorge	1.75	1.90	1.91	8.86	8.86
Mangatera	Mana_2b	Manawatū Weber Road to Tamaki Confluence	1.21	1.21	1.31	0.71	8.42
Mowhanau Estuary	West_3CMA	Mowhanau	1.17	1.21	1.24	3.98	6.60
Lower Makotuku	Whau_3c	Lower Whangaehu	1.85	1.96	1.96	6.02	6.02
Mangaatua	Mana_9c	Upper Gorge	1.50	1.58	1.59	5.46	5.95
Middle Rangitikei	Rang_2a	Middle Rangitikei	3.20	3.34	3.34	4.28	4.28
Middle Manawatū	Mana_10a	Middle Manawatū	0.73	0.73	0.75	0.08	2.37
Lower Mangatainoka	Mana_8c	Mangatainoka	2.24	2.26	2.26	0.90	0.91
Tokiahuru	Whau_1c	Upper Whangaehu	1.89	1.90	1.90	0.43	0.43
Upper Mangawhero	Whau_3d	Lower Whangaehu	1.93	1.94	1.94	0.38	0.38

Notes: If the sediment load at a river site is a fraction of the baseline, *frac*, then visual clarity (v) will increase by the ratio $frac^c$. The percentage increase in visual clarity for subzones mapped in Figure 15 are calculated as $(frac^c - 1) \times 100$. Fractions of suspended sediment concentrations are given for scenarios 0 and 3 for the year 2043. Only water management subzones are listed that (i) are impacted by SLUI works, and (ii) have an associated measurement site. Overall, 66 of 124 subzones were found to have a reduction in TSS by 2043, but only 29 of these can be characterised in terms of visual clarity due to the limited number of measurement sites.